ELSEVIER

Chemical Geology 197 (2003) 287–318

CHEMICAL GEOLOGY
INCLUDING
ISOTOPE GEOSCIENCE

www.elsevier.com/locate/chemgeo

^{40}Ar–^{39}Ar dating and geochemical characteristics of late Cenozoic basaltic rocks from the Zhejiang–Fujian region, SE China: eruption ages, magma evolution and petrogenesis

Kung-suan Ho[a], Ju-chin Chen[b,*], Ching-hua Lo[c], Hai-ling Zhao[d]

[a] *Department of Geology, National Museum of Natural Science, Taichung 404, Taiwan, ROC*
[b] *Institute of Oceanography, National Taiwan University, P.O. Box 23-13, Taipei 106, Taiwan, ROC*
[c] *Department of Geosciences, National Taiwan University, Taipei 106, Taiwan, ROC*
[d] *China University of Geosciences, Beijing 100083, China*

Received 2 May 2002; accepted 12 November 2002

Abstract

The Zhejiang–Fujian late Cenozoic volcanism took place sporadically in four volcanic belts and constitutes an important diffuse continental rift basalt province in eastern China. The volcanic rocks consist predominantly of basanite, alkali olivine basalt, olivine tholeiite and quartz tholeiite with subordinate nephelinite and rare alkali picrite basalt. Twenty-four new ages of the basaltic rocks and amphibole megacryst determined by ^{40}Ar–^{39}Ar incremental heating experiments demonstrate that the basaltic lava erupted from 0.9 to 26.4 Ma. Although some basanite dikes and nephelinite pipes in Inner and Inner Middle belts of the Zhejiang area are early Miocene, almost all the late Cenozoic basaltic volcanism occurred following cessation of South China Sea seafloor spreading ($\leq$ 16 Ma). Based on these results, most late Cenozoic intraplate magmatism surrounding the South China Sea margins may be related to the migration of the South China Sea mid-ocean ridge system beneath SE China since mid-Miocene. However, in the Zhejiang–Fujian region, volcanic activities terminated gradually and propagated westward and northward due to the collision of the Luzon arc with the eastern edge of the Eurasia continent during late Miocene to Pleistocene.

The Zhejiang–Fujian basalts exhibit trace element and isotopic affinities with OIB. Sr and Nd isotope compositions range from 0.703264 to 0.704235 and 0.512725 to 0.512961, respectively, similar to the composition of the Leiqiong basalts in South China. The enrichment of LREE coupled with depleted Sr–Nd isotopic compositions in the basaltic rocks imply that recent mantle metasomatism occurred shortly before the Cenozoic magmatism. The Sr–Nd–Pb isotopic compositions as well as high LILE/HFSE ratios found in some basaltic rocks showed that an EM2-type lead isotope signature existed in the continental lithospheric mantle in the Zhejiang–Fujian region. This character may have resulted from mantle metasomatism due to a paleo-subduction event. The Zhejiang–Fujian basaltic rocks were generated by partial melting and mixing of different proportions of depleted asthenospheric mantle (DMM or MORB) with EM2-type lithospheric mantle and have undergone different degree of fractional crystallization when the magma ascended to the surface.

Keywords: ^{40}Ar–^{39}Ar age; Petrogenesis; Magmatism; Late Cenozoic; South China

* Corresponding author. Fax: +886-2-23626092.
E-mail address: jcchen@oc.ntu.edu.tw (J. Chen).

0009-2541/02/$ - see front matter © 2002 Elsevier Science B.V. All rights reserved.
doi:10.1016/S0009-2541(02)00399-6

1. Introduction

Zhejiang, Fujian, Guangdong and Hainan provinces of SE China lie on the East Asiatic continental margin with abundant Cenozoic basalts belonging to the circum-Pacific volcanic belt. Volcanism is generally attributed to mantle upwelling induced by passive extension or asthenosphere extension following the collision of India into Eurasia, before the termination by a return to a more compressional tectonic regime (Chung et al., 1994; Smith, 1998).

According to the timing of cessation of the South China Sea floor spreading (~ 16 Ma, Chung et al., 1997), the late Cenozoic volcanic activity in SE China may be divided into two periods: (1) volcanic rocks of the 1st period (>16 Ma)—the sparse volcanic activities occurred and produced small amounts of lavas and pyroclastics. Some of the basalt lavas, basanite dikes and nephelinite pipes have been dated including the surface outcrop samples in Puning, Guangdong province, Zhejiang Inner volcanic belt and borehole samples in the northern part of Hainan Island, and radiometric ages yielded 34.3–16.3 Ma (Sun, 1991; this study). (2) Volcanic rocks of the 2nd period (≤ 16 Ma)—the eruption process of this period was particularly active, and a large amount of basaltic lavas with minor pyroclastic rocks erupted to form a diffuse volcanic province.

In Zhejiang–Fujian area, the volcanic rocks are mainly distributed near the coastal area, including Shengxian, Xinchang, Ninghai, Linhai and Longhai. Occurrences of basaltic rocks in other areas are generally small and scattered (Fig. 1). Development of these volcanic rocks might have been essentially controlled by a series of northeast–southwest trending fault system, where many isolated tectono-volcanic basins, calderas and volcanic rents of different sizes occurred. According to the relation between the volcanic rock crop out and deep fault distribution (Bureau of Geology and Mineral Resources of Zhejiang Province, 1989; Bureau of Geology and Mineral Resources of Fujian Province, 1985), four NE trending volcanic belts can be divided from east to west (Fig. 1), namely, Xiamen–Longhai–Dongshan belt (Outer belt), Ninghai–Linhai–Minqing–Puning belt (Outer Middle belt), Shengxian, Xinchang–Jinyun–Songxi–Yongding belt (Inner Middle belt), Zhuji–Longyou–Quzhou belt (Inner belt of Zhejiang) and Mingxi–Qingliu–Changting belt (Inner belt of Fujian). Based on the geophysical data (Ma and Wu, 1987), the crustal and lithospheric thickness gradually increased from the coastal to inland areas.

Previous age dating for late Cenozoic basaltic rock in Zhejiang–Fujian area was mainly by K–Ar method (Wang and Yang, 1987; Liu et al., 1992). Although more than 10 age data of the Zhejiang basaltic rocks have been published in the last two decades, whereas the K–Ar age determinations on the basaltic specimens were mainly concentrated in the Shengxian and Xinchang regions. The virtual absence of age data in some volcanic regions such as Inner belt of Zhejiang province has limited the study of the magmatic evolution. In addition, it is worth noting that the Ar–Ar ages of the basaltic rocks in some regions are always younger than the ages obtained by the K–Ar method. Owing to some problems in dating volcanic rocks by the K–Ar method, e.g., loss of Ar or gain of K associated with alteration and inherited argon residing in phenocryst can be overcome by the ^{40}Ar–^{39}Ar technique (Lo et al., 1994). Therefore, we used ^{40}Ar–^{39}Ar method to determine the eruption ages of basaltic rocks from four volcanic belts in the Zhejiang–Fujian region.

In addition, we report the major and trace element abundances, and Sr–Nd isotope data for basaltic rocks from Zhejiang–Fujian volcanic province. These results are used to (1) determine the temporal and spatial distribution of the volcanic activity, and (2) identify the geochemical characteristics of the magma source regions and understand the genesis of late Cenozoic basalts. Besides, the Zhejiang–Fujian region offers a good opportunity to investigate the route of magma migration that is essentially intraplate in origin, being formed after the cessation of the South China Sea

Fig. 1. Map of the SE China showing major outcrops of late Cenozoic extension-related basaltic rocks and sample sites in Zhejiang–Fujian area. Four volcanic belts: 1A, Inner belt of Zhejiang; 1B, Inner belt of Fujian; 2, Inner Middle belt; 3, Outer Middle belt; 4, Outer belt are also shown. Distribution of basaltic rocks modified after Bureau of Geology and Mineral Resources of Zhejiang Province (1989) and Bureau of Geology and Mineral Resources of Fujian Province (1985).

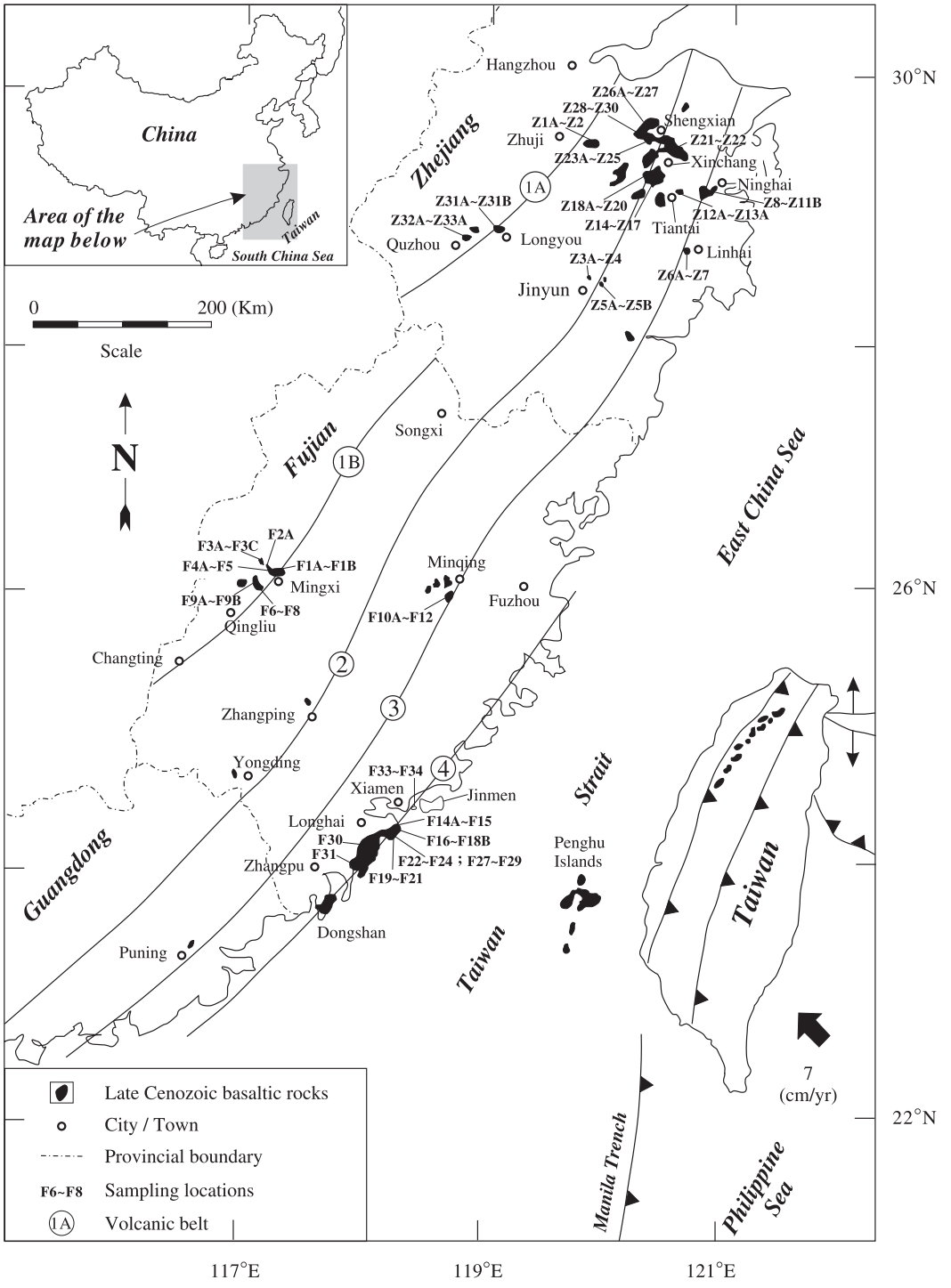
China
Area of the map below
Taiwan
South China Sea
0
200 (Km)
Scale
N
Hangzhou
Zhejiang
Fujian
Guangdong
Songxi
Mingxi
Qingliu
Changting
Zhangping
Yongding
Longhai
Zhangpu
Puning
Dongshan
Xiamen
Jinmen
Minqing
Fuzhou
Quzhou
Longyou
Zhuji
Shengxian
Xinchang
Ninghai
Tiantai
Linhai
Jinyun
Penghu Islands
Strait
East China Sea
Taiwan
Manila Trench
Philippine Sea
Z26A~Z27
Z28~Z30
Z1A~Z2
Z21~Z22
Z23A~Z25
Z31A~Z31B
Z32A~Z33A
Z18A~Z20
Z14~Z17
Z12A~Z13A
Z8~Z11B
Z3A~Z4
Z6A~Z7
Z5A~Z5B
F3A~F3C
F2A
F4A~F5
F1A~F1B
F9A~F9B
F6~F8
F10A~F12
F33~F34
F14A~F15
F30
F16~F18B
F31
F22~F24 ; F27~F29
F19~F21
1A
1B
2
3
4
7
(cm/yr)
30°N
26°N
22°N
117°E
119°E
121°E
Late Cenozoic basaltic rocks
City / Town
Provincial boundary
F6~F8 Sampling locations
1A Volcanic belt

seafloor spreading in mid-Miocene. Therefore, we combine the radiometric age and geochemical data to monitor the migration route of the late Cenozoic magmatism in SE China.

2. Analytical methods

Twenty-three basaltic rocks and one amphibole megacryst were dated by $^{40}Ar/^{39}Ar$ incremental heating method. Samples were carefully selected to avoid alteration, on the bases of petrographic examination and chemical composition, which shows low loss-on-ignition content (L.O.I. < 3 wt.%). An 80–120-mesh sieve-sized fraction of the samples was chosen and ultrasonically cleaned in acetone and distilled water baths. Weighted aliquots of samples (0.5104–1.6021 g) were wrapped in aluminum foil packet and stacked in aluminum canister with LP-6 biotite standard (127.7 ± 1.4 Ma, Odin et al., 1982) and HDB-1 biotite (24.7 ± 0.4 Ma, Fuhrmann et al., 1987), and irradiated in position VT-C of the THOR Reactor, with neutron flux of 1.566×10^{13} n/cm^2 s, at National Tsing-Hua University for 8 h. After irradiation, samples were loaded in degassed fused silica boats, and placed into a degassed fused quartz tube, baked at 250 °C for 24 h, and then incrementally heated following a 30-min per step schedule using a resistance furnace. The purified gas was analyzed with a Varian-MAT GD150 mass spectrometer. The concentrations of ^{36}Ar, ^{37}Ar, ^{38}Ar, ^{39}Ar and ^{40}Ar were corrected for system blanks, for radioactive decay of the nucleogenic isotopes, and for minor interference reactions involving Ca, K and Cl, following procedures outlined in detail by Lo and Lee (1994). The gradient of the neutron flux across the irradiated canister was less than 0.5% as reflected in the *J*-value variation between the standards at the top and the bottom of the canister. A weighted mean of *J* values obtained from the analyses of irradiation standard minerals is adopted in the age calculations. Integrated dates were calculated from the sum total of the peak heights and their errors from the square root of the sum of squares of the peak height errors, for all of the temperature steps. Plateau dates were calculated by the same approach, but utilizing only those temperature steps yielding dates on the plateau. As discussed by Lanphere and Dalrymple (1978), a plateau should meet the following three requirements: (1) at least four successive temperature steps with dates that fall within 2σ of the average; (2) the gas fractions for these plateau steps, which must comprise more than 50% of total ^{39}Ar released; and (3) the plateau date should be concordant with its respective intercept date, with reasonable $^{40}Ar/^{36}Ar$ intercept value, obtained from the isotope correlation plots. Data were further plotted on age spectra and $^{36}Ar/^{40}Ar$–$^{39}Ar/^{40}Ar$ isotope correlation diagrams. The $^{40}Ar/^{39}Ar$ dates and $^{40}Ar/^{36}Ar$ intercept values were calculated from the intercept of the regressed line, respectively. The cubic least-square fitting scheme outlined by York (1969) was employed in regressing the data. Because the $^{39}Ar_K$, $^{38}Ar_{Cl}$ and $^{37}Ar_{Ca}$ release data potentially reflect the chemical compositions (K, Cl and Ca, respectively) of the samples, the data are also plotted as Ca/K and Cl/K spectra for each sample. Ca/K and Cl/K ratios are calculated according to the relationships $Ca/K = 1.82\ (\pm 0.17) \times {}^{37}Ar_{Ca}/{}^{39}Ar_K$ and $Cl/K = 0.22\ (\pm 0.04) \times {}^{38}Ar_{Cl}/{}^{39}Ar_K$, as described by Lo and Lee (1994). The detailed $^{40}Ar/^{39}Ar$ analytical data are available on request from the senior author.

A set of 85 samples was analyzed for major and trace element abundances. All elements except Si and Al were determined using solutions prepared by dissolving 0.5 g of rock powder in a mixture of ultrapure HF and HNO_3 in Teflon beakers under clean room condition. Solutions were analyzed using a Perkin-Elmer Model 5100PC atomic absorption spectrophotometer (Fe, Mg, Ca, Na, K, Mn, Co, Cr, Cu, Li, Ni, Rb, Sr, Zn) and inductively coupled plasma mass spectrometry (Ba, Hf, Nb, Sc, Th, V, Y, Zr, La, Ce, Nd, Sm, Eu, Gd, Tb, Dy, Yb, Lu) at National Museum of Natural Science and National Tsing-Hua University. For Si and Al determinations, the solutions were prepared by NaOH fusion of 0.05 g rock powder in nickel crucibles followed by water leaching and HCl acidification. The analyses of Si, Al, Ti and P were carried out by the colorimetric method using an SP-2000 spectrophotometer at the National Taiwan University. Calibration curves were constructed using US Geological Survey rock standards AGV-1, BCR-1, W-1 and G-2 and Geological Survey of Japan rock standard JB-1. Values for these rock standards were adapted from compilations by Govindaraju (1994). The precision is estimated to be around ± 2% for atomic absorption and colorimetric methods and better than ± 5% for all ICP-MS analyses (Table 1). The

Table 1
Precision test for international rock standard W-1

Element	Analytical method[a]	Literature value[b]	Replicate analyses by present study					Average value[c]	S.D.[d]	C.V.[e] (%)
			W101	W102	W103	W104	W105			
(wt.%)										
ΣFeO	1	10.05	9.97	9.91	10.23	9.87	9.81	9.96	0.15	1.46
MgO	1	6.62	6.55	6.54	6.44	6.59	6.67	6.56	0.08	1.14
CaO	1	10.99	11.23	11.15	10.82	10.78	10.78	10.95	0.20	1.79
Na_2O	1	2.16	2.13	2.14	2.18	2.18	2.16	2.16	0.020	0.95
K_2O	1	0.64	0.64	0.63	0.65	0.66	0.65	0.65	0.010	1.58
MnO	1	0.17	0.165	0.164	0.168	0.172	0.171	0.168	0.003	1.88
(ppm)										
Li	1	12.8	12.3	12.3	12.8	12.8	12.7	12.6	0.23	1.84
Cr	1	119	116	115	118	120	121	118	2.28	1.93
Cu	1	113	110	113	113	111	112	112	1.17	1.04
Zn	1	84	87	85	86	84	84	86	1.17	1.37
Rb	1	21.4	22.1	21.9	21.1	21.2	22.0	21.7	0.42	1.95
Sr	1	186	185	188	183	182	186	185	2.14	1.16
Y	2	26	25	25	24	24	25	25	0.49	1.99
Nb	2	9.9	10.1	9.4	9.1	9.7	9.1	9.5	0.38	4.03
Ba	2	162	166	161	165	163	162	163	1.86	1.14
La	2	11	10.8	11.0	10.9	10.6	10.7	10.8	0.14	1.31
Ce	2	23.5	23.7	23.0	23.6	22.8	23.3	23.3	0.34	1.47
Nd	2	14.6	14.8	15.2	14.6	14.0	14.7	14.7	0.39	2.65
Sm	2	3.68	3.45	3.55	3.53	3.44	3.56	3.51	0.051	1.45
Eu	2	1.12	1.15	1.13	1.13	1.09	1.09	1.12	0.024	2.15
Tb	2	0.63	0.67	0.67	0.64	0.62	0.63	0.64	0.021	3.19
Yb	2	2.03	2.17	2.15	2.18	2.07	2.09	2.13	0.044	2.06
Lu	2	0.317	0.35	0.35	0.32	0.34	0.33	0.34	0.012	3.45
Hf	2	2.5	2.3	2.6	2.4	2.5	2.4	2.4	0.10	4.18
Th	2	2.4	2.5	2.6	2.5	2.4	2.4	2.5	0.08	3.02

[a] Present study: 1, AAS; 2, ICP-MS.
[b] Govindaraju (1994).
[c] Present study.
[d] Standard deviation $= \sqrt{\frac{1}{N}\sum_{i=1}^{n}(X_i - \overline{X})^2}$.
[e] Coefficient of variation=(S.D./$\overline{X}$) × 100.

details of the analytical techniques have been discussed by Ho (1998).

Eleven representative basaltic rocks were analyzed for Sr–Nd isotopic composition following the procedure of Smith and Huang (1997). Isotopic compositions were measured using a MAT 262 mass spectrometer at National Cheng Kung University. Nd isotopic ratios have been normalized to $^{146}Nd/^{144}Nd = 0.7219$ and are reported relative to 0.511855 for the La Jolla standard. Sr isotopic ratios are normalized to $^{86}Sr/^{88}Sr = 0.1194$ and are relative to 0.710240 for the SRM987 standard. Precision of Nd and Sr isotopic compositions is better than ± 0.000010 (2σ).

3. Petrography and principal rock types

Basaltic lava flow is the major type of volcanic activities in Zhejiang–Fujian region, and sometimes basanitic dikes or breccia pipes also occurred. The basaltic rocks are mostly massive, and exhibit porphyric, fine granular and aphyric textures. The phenocrysts consist predominantly of lath plagioclase and interstitial clinopyroxene in tholeiite; of clinopyroxene, olivine and plagioclase in alkali olivine basalt; and of olivine and clinopyroxene in basanite, alkali picrite basalt and nephelinite. The groundmass in tholeiite and alkali olivine basalt is rather variable,

and is mainly composed of fine- to medium-grained plagioclase, clinopyroxene, olivine and Fe–Ti oxide minerals. Nephelinites and a few basanites with essentially no feldspar phase, but with abundant nepheline and accessory analcite, occur as pipe or lava flow. In addition, alkali feldspar is present in minor amount in most of the alkali basalts.

Based on Ne–Ol–Di–Hy–Qz tetrahedron of Yoder and Tilley (1962), the basaltic rocks can be classified into three types, e.g., quartz tholeiite, olivine tholeiite and alkali basalt (Fig. 2A). The chemical compositions of the Zhejiang–Fujian alkali basalts vary considerably (e.g., $SiO_2 = 39.62–50.33$ wt.%, $Na_2O + K_2O = 2.52–7.83$ wt.%, Table 2), accordingly

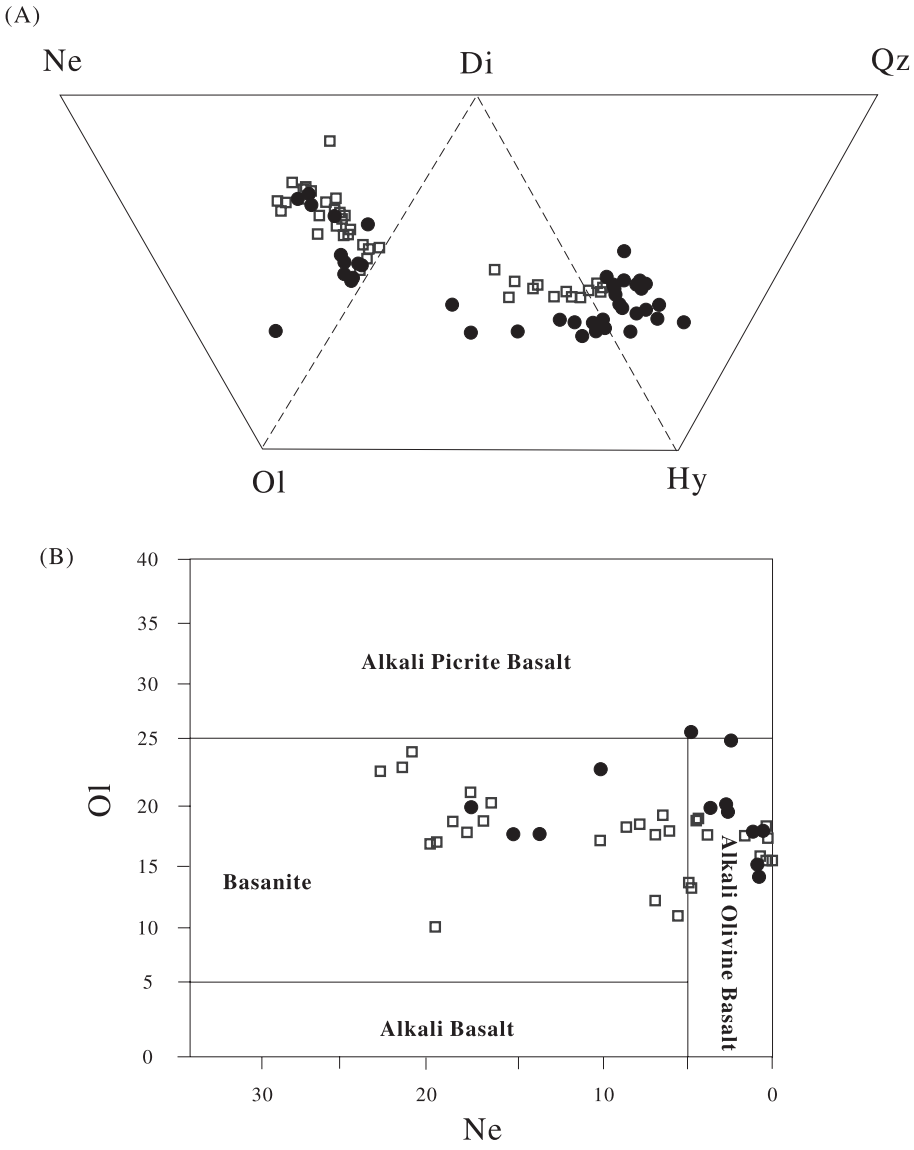

Fig. 2. (A) Normative compositions of basaltic rocks from the Zhejiang–Fujian area. Nomenclature of volcanic rocks after Yoder and Tilley (1962). (B) Plots of normative nepheline against normative olivine compositions for alkali basalts. Field boundaries after Chih (1988). Zhejiang basalts are indicated by the unfilled squares, Fujian basalts by filled circles.

Table 2
Major and trace element compositions of representative basaltic rocks from Zhejiang–Fujian area

Province	Zhejiang								
Volcanic belt	Outer Middle					Inner Middle			
Locality	Linhai		Ninghai			Jinyun		Tiantai	Xinchang
Sample no.	Z-6A	Z-7	Z-8	Z-10	Z-11B	Z-3A	Z-5A	Z-12B	Z-15
Rock type[a]	OT	QT	OT	OT	QT	B	N	B	B
(wt.%)									
SiO_2	49.47	50.86	49.22	50.19	50.79	45.42	42.04	41.51	48.66
Al_2O_3	13.60	13.87	13.62	13.41	13.65	12.33	11.46	12.12	14.60
ΣFeO[b]	11.86	11.34	10.90	11.14	10.65	12.21	14.36	13.65	11.34
MgO	7.35	6.85	8.27	7.85	7.32	9.95	6.94	10.38	3.50
CaO	9.53	9.36	9.05	9.28	9.09	10.82	12.95	11.19	6.65
Na_2O	2.92	2.87	2.93	2.86	2.85	3.06	4.30	4.11	4.38
K_2O	0.98	0.84	1.02	0.88	0.65	1.77	2.31	1.25	3.45
TiO_2	2.92	2.66	2.50	2.58	2.16	2.60	2.77	2.91	2.44
P_2O_5	0.64	0.48	0.43	0.44	0.30	0.82	1.48	0.84	1.12
MnO	0.154	0.154	0.159	0.163	0.166	0.180	0.236	0.206	0.169
L.O.I.	0.70	0.39	1.34	1.31	1.69	1.19	0.96	1.74	2.95
Total	100.124	99.674	99.439	100.103	99.316	100.350	99.806	99.906	99.259
MG[c]	57.99	57.37	62.83	61.09	60.49	64.48	51.85	62.88	40.74
(ppm)									
Li	4.5	4.5	6.1	4.9	8.3	13.0	22.5	9.8	33.6
Sc	21.2	21.3	21.0	22.1	20.8	18.8	14.6	19.7	9.4
V	182	171	155	158	167	191	144	208	78
Cr	226	220	286	263	234	272	122	224	36
Co	56.3	50.7	51.1	51.2	48.4	61.3	49.5	61.4	36.3
Ni	168	135	199	185	151	233	107	180	51
Cu	91	75	76	69	65	137	43	62	29
Zn	114	114	166	113	108	113	183	130	190
Rb	18.2	15.7	15.5	9.3	6.5	49.4	49.7	40.9	4.47
Sr	502	487	535	574	420	924	1948	1167	1621
Y	25	24	24	25	21	25	44	29	38
Zr	143	139	157	172	123	156	322	209	406
Nb	18.9	18.0	19.9	21.9	14.7	37.7	91.9	60.3	80.9
Ba	295	238	273	285	211	601	737	691	945
La	16.0	13.6	18.2	19.3	11.9	37.5	83.2	45.3	62.8
Ce	36.6	31.1	38.3	40.1	25.8	68.7	154.1	81.8	117.7
Nd	26.0	22.3	25.9	27.8	17.8	36.1	81.8	46.1	69.8
Sm	7.36	6.72	7.35	7.94	5.55	7.94	17.69	11.08	17.49
Eu	2.64	2.54	2.73	3.09	2.16	2.59	6.58	4.45	7.29
Tb	0.65	0.68	0.71	0.77	0.70	0.61	0.92	0.89	1.10
Yb	1.43	1.57	1.66	1.85	1.73	1.33	1.84	1.88	2.11
Lu	0.20	0.26	0.27	0.31	0.29	0.12	0.24	0.30	0.38
Hf	4.0	4.3	5.1	5.8	4.2	3.6	8.5	6.8	12.6
Th	1.4	1.6	2.6	2.8	2.1	5.1	11.5	7.1	10.2
U	0.82	1.24	1.66	1.80	1.89	1.24	3.07	3.16	4.90
Ba/Rb	16.2	15.2	17.6	30.7	32.5	12.2	14.8	16.9	211.4
Zr/Nb	7.6	7.7	7.9	7.9	8.4	4.1	3.5	3.5	5.0
Zr/Y	5.7	5.8	6.5	6.9	5.9	6.2	7.3	7.2	10.7
La/Ce	0.44	0.44	0.48	0.48	0.46	0.56	0.54	0.55	0.53
Ce/Sm	5.0	4.6	5.2	5.1	4.7	8.7	8.7	7.4	6.7
$(La/Yb)_N$	8.0	6.2	7.9	7.5	4.9	20.2	32.4	17.3	21.4

(continued on next page)

Table 2 (*continued*)

Province	Zhejiang								
Volcanic belt	Inner Middle								
Locality	Xinchang						Shengxian		
Sample no.	Z-16	Z-18A	Z-19	Z-20	Z-21	Z-22	Z-23A	Z-24	Z-25
Rock type[a]	B	AOB	OT	B	AOB	QT	OT	OT	B
(wt.%)									
SiO_2	44.45	47.24	50.86	40.80	48.56	50.92	51.99	51.23	39.62
Al_2O_3	14.70	14.52	14.28	11.92	13.53	14.20	14.12	13.89	11.87
ΣFeO[b]	12.11	11.29	10.99	13.64	11.60	10.68	11.24	10.86	13.89
MgO	7.66	7.65	7.04	11.08	8.52	6.52	6.99	7.15	10.43
CaO	9.28	9.14	8.92	11.05	9.13	8.89	8.78	8.94	11.07
Na_2O	3.43	3.01	3.04	3.91	3.35	3.09	3.40	3.39	3.64
K_2O	1.65	1.53	1.17	1.15	1.21	0.70	1.24	1.15	1.14
TiO_2	2.66	2.38	2.05	2.69	2.41	2.07	2.18	2.10	2.85
P_2O_5	0.69	0.59	0.35	1.09	0.47	0.36	0.39	0.38	1.19
MnO	0.171	0.187	0.160	0.205	0.178	0.168	0.16	0.16	0.217
L.O.I.	2.77	2.22	0.77	2.03	1.30	2.60	0.01	0.15	3.53
Total	99.571	99.757	99.630	99.565	100.258	100.198	100.50	99.40	99.447
MG[c]	58.49	60.15	58.80	64.41	62.07	57.63	58.08	59.46	62.59
(ppm)									
Li	26.3	5.7	4.6	10.0	6.8	7.5	7.0	7.1	12.4
Sc	16.9	18.3	20.3	14.9	18.5	19.5	20.0	20.5	14.6
V	176	181	179	169	169	168	185	182	177
Cr	175	182	188	281	244	212	184	183	222
Co	51.8	50.2	49.3	59.8	53.5	45.3	51.1	50.8	60.0
Ni	162	126	121	244	188	123	148	148	202
Cu	82	60	74	70	75	69	79	75	72
Zn	141	117	110	141	113	111	120	116	159
Rb	31.8	32.9	22.1	41.2	23.5	11.1	18.6	17.3	27.7
Sr	1036	678	502	1402	641	496	503	527	1250
Y	28	24	22	26	21	22	24	23	29
Zr	260	167	133	211	122	124	130	120	242
Nb	62.0	39.7	23.4	71.8	27.4	20.5	21.7	21.3	83.5
Ba	559	432	263	697	334	264	301	305	218
La	38.5	26.2	17.6	47.9	20.7	17.2	15.5	15.2	57.1
Ce	75.1	51.0	35.6	90.3	40.0	33.5	31.6	30.5	101.9
Nd	38.2	26.4	19.7	45.1	22.0	19.0	18.5	18.2	52.3
Sm	8.74	6.14	4.98	9.68	5.37	5.14	5.01	5.00	10.95
Eu	2.83	2.04	1.66	3.09	1.75	1.69	1.71	1.77	3.41
Tb	1.18	0.92	0.81	1.32	0.88	0.85	0.89	0.88	1.37
Yb	1.59	1.54	1.48	1.58	1.57	1.58	1.67	1.71	1.52
Lu	0.22	0.22	0.21	0.25	0.25	0.24	0.24	0.29	0.19
Hf	5.8	3.8	3.1	5.0	3.1	3.3	3.3	3.2	5.7
Th	6.0	4.2	2.8	8.0	3.1	2.6	2.2	2.2	8.8
U	1.50	1.03	0.65	2.01	0.88	0.65	0.59	0.84	2.23
Ba/Rb	17.6	13.1	11.9	16.9	14.2	23.8	16.2	17.6	7.9
Zr/Nb	4.2	4.2	5.7	2.9	4.5	6.1	6.0	5.6	2.9
Zr/Y	9.3	7.0	6.1	8.1	5.8	5.6	5.4	5.2	8.3
La/Ce	0.51	0.51	0.49	0.53	0.52	0.51	0.49	0.50	0.56
Ce/Sm	8.6	8.3	7.2	9.3	7.5	6.5	6.3	6.1	9.3
$(La/Yb)_N$	17.4	12.2	8.5	21.8	9.5	7.8	6.7	6.4	27.0

Table 2 (*continued*)

Province	Zhejiang							Fujian	
Volcanic belt	Inner Middle		Inner					Inner	
Locality	Shengxian		Zhuji		Longyou	Quzhou		Mingxi	
Sample no.	Z-26A	Z-28B	Z-1A	Z-1C	Z-31B	Z-32A	Z-33A	F-1B	F-2A
Rock type[a]	AOB	AOB	B	AOB	B	N	N	N	N
(wt.%)									
SiO_2	50.33	49.27	46.86	46.62	42.51	40.56	39.57	41.4	43.35
Al_2O_3	13.53	14.50	13.68	13.17	13.52	11.22	11.67	12.7	12.52
ΣFeO[b]	10.83	10.53	11.60	12.01	11.50	12.42	13.34	12.8	11.64
MgO	7.44	6.35	8.83	8.85	9.43	12.07	9.69	9	11.45
CaO	8.66	8.30	9.90	9.48	10.12	11.23	11.15	11.2	10.75
Na_2O	3.78	4.13	3.37	3.29	4.57	5.03	3.91	3	3.92
K_2O	1.50	2.34	1.78	1.58	1.84	2.21	1.44	2	2.20
TiO_2	2.31	2.86	2.34	2.29	2.50	2.47	3.12	3	2.47
P_2O_5	0.56	0.79	0.70	0.59	0.91	1.42	1.38	1	1.14
MnO	0.156	0.154	0.17	0.177	0.175	0.194	0.184	0.1	0.18
L.O.I.	0.31	0.42	0.72	1.35	2.39	0.63	4.23	1	0.14
Total	99.406	99.644	99.95	99.407	99.465	99.454	99.684	9.9	99.76
MG[c]	60.48	57.33	62.91	62.15	64.62	68.41	61.81	63.20	68.67
(ppm)									
Li	9.0	11.5	7.3	8.1	15.2	15.9	109.7	14.5	9.1
Sc	18.3	15.1	17.3	18.5	18.7	14.0	15.5	21.6	19.0
V	178	216	179	179	165	156	143	188	160
Cr	217	48	227	225	212	373	208	159	326
Co	48.8	40.4	56.2	53.5	52.5	57.3	59.8	62.3	57.4
Ni	179	76	194	192	190	330	186	182	307
Cu	62	65	80	79	54	46	64	52	56
Zn	117	122	121	116	122	143	137	138	112
Rb	28.9	47.8	33.8	27.8	21.5	38.4	25.9	87.8	62.5
Sr	633	901	788	762	1318	1539	1384	1604	1302
Y	24	31	23	24	29	32	32	38	30
Zr	156	234	157	157	261	320	293	387	301
Nb	33.7	55.2	39.1	40.1	96.9	157.2	116.5	48.0	52.7
Ba	388	695	473	462	937	956	77	1068	965
La	22.0	35.0	25.7	25.1	64.3	98.0	89.4	97.5	81.1
Ce	43.0	66.6	49.3	47.7	117.6	164.6	150.5	179.7	145.8
Nd	23.9	33.5	24.9	25.3	55.3	67.8	86.5	86.4	65.8
Sm	6.08	8.07	6.29	6.01	10.72	13.20	16.62	15.69	11.62
Eu	2.01	2.68	2.27	2.03	3.39	4.29	4.58	3.67	2.89
Tb	0.93	1.17	0.65	0.57	1.27	1.60	1.46	1.83	1.42
Yb	1.62	1.98	1.43	1.28	1.72	1.70	2.00	2.91	2.22
Lu	0.20	0.28	0.22	0.18	0.21	0.21	0.20	0.38	0.30
Hf	3.8	5.3	3.9	3.6	5.8	7.2	9.8	7.9	6.2
Th	3.8	5.6	3.9	3.2	10.4	16.2	13.9	13.2	12.0
U	0.79	1.29	1.56	0.88	2.32	3.56	3.01	2.99	2.64
Ba/Rb	13.4	14.5	14.0	16.6	43.6	24.9	3.0	12.2	15.4
Zr/Nb	4.6	4.2	4.0	3.9	2.7	2.0	2.5	8.1	5.7
Zr/Y	6.5	7.6	6.8	6.5	9.0	10.0	9.2	10.2	10.0
La/Ce	0.51	0.53	0.52	0.53	0.55	0.60	0.59	0.54	0.56
Ce/Sm	7.1	8.3	7.8	7.9	11.0	12.5	9.1	11.5	12.6
$(La/Yb)_N$	9.7	12.7	12.9	14.1	26.8	41.4	32.1	24.0	26.2

(continued on next page)

Table 2 (*continued*)

Province	Fujian								
Volcanic belt	Inner					Outer Middle			Outer
Locality	Mingxi				Qingliu	Minqing			Longhai
Sample no.	F-3A	F-4A	F-5	F-9B	F-6	F-10B	F-11	F-12	F-14B
Rock type[a]	QT	APB	AOB	OT	OT	AOB	AOB	AOB	QT
(wt.%)									
SiO_2	53.92	42.01	46.87	51.85	51.75	48.01	47.81	47.58	52.13
Al_2O_3	14.34	11.98	12.95	14.48	14.15	13.15	13.40	13.25	15.41
ΣFeO[b]	9.64	12.15	11.29	9.68	9.61	9.52	9.69	10.24	9.96
MgO	6.60	13.08	9.93	7.23	8.09	10.46	9.06	9.68	5.09
CaO	8.53	11.57	9.26	8.08	7.95	8.95	9.05	8.96	7.75
Na_2O	3.05	1.34	2.99	3.25	3.11	2.94	2.58	2.71	3.24
K_2O	1.04	1.18	1.93	1.20	1.25	2.19	2.51	2.50	1.61
TiO_2	1.87	2.87	2.66	1.88	1.88	2.04	2.06	2.11	1.95
P_2O_5	0.40	1.11	0.84	0.47	0.54	0.79	0.81	0.84	0.54
MnO	0.131	0.188	0.174	0.130	0.152	0.156	0.147	0.15	0.128
L.O.I.	0.66	3.31	0.63	0.88	1.35	1.65	2.83	1.67	1.80
Total	100.281	100.788	99.524	99.130	99.832	99.856	99.947	99.59	99.608
MG[c]	60.40	70.57	66.21	62.46	65.22	71.00	67.56	67.80	53.24
(ppm)									
Li	4.8	8.1	7.7	7.3	6.6	8.1	6.1	7.1	3.6
Sc	17.9	19.3	21.0	17.7	17.9	16.9	17.6	18.0	16.8
V	116	174	174	127	128	139	143	127	129
Cr	257	369	272	294	332	386	372	322	130
Co	48.5	62.3	61.8	42.2	80.2	49.4	49.1	49.0	37.7
Ni	176	333	251	207	250	304	287	252	95
Cu	71	52	58	81	85	67	65	62	53
Zn	103	118	120	114	143	106	109	109	142
Rb	17.6	127.3	44.1	25.4	25.6	65.9	60.3	55.9	48.7
Sr	513	1560	971	522	561	1181	1134	1191	570
Y	22	32	27	29	23	25	26	24	22
Zr	138	307	239	153	163	279	296	247	226
Nb	16.3	90.6	78.5	27.6	38.1	68.4	67.0	69.8	43.0
Ba	272	903	710	333	361	850	774	735	428
La	20.8	85.1	56.6	32.3	29.6	58.8	58.9	53.0	32.4
Ce	41.3	154.2	106.5	49.4	58.3	110.0	110.9	100.2	59.9
Nd	23.1	73.7	52.4	38.8	29.5	50.5	52.5	55.0	33.9
Sm	5.57	13.19	9.84	9.26	6.40	9.34	9.79	10.32	7.70
Eu	1.04	2.26	2.49	2.32	1.59	1.70	1.77	2.80	2.43
Tb	0.74	1.59	1.17	1.20	0.80	1.12	1.21	0.97	0.91
Yb	1.65	2.33	2.05	2.37	1.64	1.86	2.00	1.52	1.31
Lu	0.24	0.31	0.26	0.30	0.24	0.24	0.23	0.20	0.17
Hf	3.4	6.0	5.9	3.6	4.0	5.9	6.3	6.5	5.7
Th	3.0	10.4	7.9	3.3	4.8	9.3	8.2	7.5	4.0
U	0.74	1.92	1.74	0.86	1.13	2.25	2.06	1.83	0.83
Ba/Rb	15.5	7.1	16.1	13.1	14.1	12.9	12.8	13.2	8.8
Zr/Nb	8.5	3.4	3.0	5.5	4.3	4.1	4.4	3.5	5.3
Zr/Y	6.3	9.6	8.9	5.3	7.1	11.2	11.4	10.3	10.3
La/Ce	0.50	0.55	0.53	0.65	0.51	0.53	0.53	0.53	0.54
Ce/Sm	7.4	11.7	10.8	5.3	9.1	11.8	11.3	9.7	7.8
$(La/Yb)_N$	9.0	26.2	19.8	9.8	13.0	22.7	21.1	25.0	17.7

Table 2 (*continued*)

Province	Fujian								
Volcanic belt	Outer								
Locality	Longhai					Zhangpu		Jinmen	
Sample no.	F-18A	F-20	F-22	F-24	F-28	F-30	F-31	F-33	F-34
Rock type[a]	OT	OT	QT	AOB	QT	OT	QT	QT	QT
(wt.%)									
SiO_2	52.09	49.15	53.60	50.01	53.74	50.58	50.79	53.30	52.50
Al_2O_3	15.21	14.60	15.38	15.31	15.89	14.98	14.92	14.86	15.38
ΣFeO[b]	9.89	10.27	9.17	9.98	8.99	9.86	10.44	9.59	10.03
MgO	6.46	7.77	7.11	6.43	6.45	7.10	5.98	7.15	7.34
CaO	7.32	8.61	8.02	7.57	9.31	7.56	7.49	9.59	9.33
Na_2O	3.24	2.88	2.71	3.55	2.58	3.13	2.94	2.72	2.75
K_2O	2.04	1.80	0.64	2.54	0.39	2.00	1.55	0.89	0.48
TiO_2	1.97	2.00	1.21	2.12	1.20	2.10	2.46	1.70	1.49
P_2O_5	0.52	0.43	0.19	0.59	0.14	0.52	0.59	0.24	0.19
MnO	0.129	0.137	0.121	0.122	0.129	0.131	0.145	0.148	0.151
L.O.I.	0.54	2.20	1.36	1.52	0.66	2.18	1.99	0.21	0.34
Total	99.409	99.847	99.511	99.742	99.479	100.141	99.295	100.398	99.981
MG[c]	59.27	62.76	63.33	58.94	61.51	61.60	56.07	62.42	61.98
(ppm)									
Li	5.1	4.3	3.0	6.3	3.0	6.5	4.7	5.0	4.0
Sc	16.2	22.6	21.0	15.4	22.1	15.9	19.5	21.8	22.6
V	141	181	133	153	125	125	154	154	153
Cr	222	268	258	120	207	230	175	228	206
Co	41.6	47.5	45.7	46.0	46.4	46.0	59.5	52.1	51.0
Ni	151	175	157	119	139	151	185	200	197
Cu	48	58	54	40	84	54	46	73	72
Zn	116	101	86	120	84	113	129	108	103
Rb	40.1	46.8	15.0	62.7	8.2	51.9	36.2	17.0	11.0
Sr	645	543	254	764	261	614	606	301	257
Y	19	22	14	22	16	21	28	20	21
Zr	245	216	98	268	91	235	281	122	112
Nb	30.6	43.2	16.2	52.4	13.2	55.2	46.2	17.5	15.6
Ba	533	466	158	587	137	521	371	163	129
La	37.5	33.9	11.6	45.4	8.9	38.8	31.5	12.6	9.7
Ce	72.0	65.0	23.1	91.2	19.0	70.3	65.8	26.2	21.2
Nd	36.1	29.7	11.8	39.7	11.6	33.7	37.1	15.9	13.4
Sm	6.98	5.90	3.43	7.71	3.28	6.64	8.01	4.00	3.50
Eu	2.01	2.37	1.22	2.97	1.19	2.05	2.17	1.38	1.21
Tb	0.71	0.85	0.47	0.95	0.49	0.85	0.98	0.65	0.61
Yb	1.30	1.47	1.07	1.37	1.15	1.38	1.55	1.66	1.56
Lu	0.13	0.17	0.12	0.17	0.14	0.18	0.23	0.21	0.20
Hf	6.2	4.9	2.1	5.9	2.3	5.9	6.3	2.9	2.7
Th	4.3	4.5	1.7	5.8	1.1	4.7	3.1	1.3	1.0
U	1.05	0.91	0.37	1.35	0.24	1.08	0.79	0.50	0.39
Ba/Rb	13.3	10.0	10.5	9.4	16.7	10.0	10.3	9.6	11.7
Zr/Nb	8.0	5.0	6.1	5.1	6.9	4.3	6.1	7.0	7.2
Zr/Y	12.9	9.8	7.0	12.2	5.7	11.2	10.0	6.1	5.3
La/Ce	0.52	0.52	0.50	0.50	0.47	0.55	0.48	0.48	0.46
Ce/Sm	10.3	11.0	6.7	11.8	5.8	10.6	8.2	6.6	6.1
$(La/Yb)_N$	20.7	16.5	7.8	23.8	5.6	20.2	14.6	5.4	4.5

based on CIPW normative data; they can be further subdivided into alkali olivine basalt, basanite, alkali picrite basalt and nephelinite (without normative albite) by the classification scheme proposed by Chih (1988) (Fig. 2B). In a survey of 85 samples (only 45 representative samples are presented in Table 2), the most abundant rock type is quartz tholeiite which constitutes about 27% of the rock samples recovered. The olivine tholeiite, alkali olivine basalt and basanite comprise about 25%, 20% and 18%, respectively, of the total samples. Only few samples analyzed fall within the nephelinite (9%) and alkali picrite basalt (1%) fields. Nephelinite and alkali picrite basalt occur as small isolated pipe or dike, and are only found in the Inner and Inner Middle belts.

In the Zhejiang province, tholeiitic rocks appear to be the most voluminous in the Outer Middle belt, but alkali basalts are the dominant type in the Inner Middle- and Inner belts. It is obvious that there is a general tendency of increase in alkali contents from the coastal areas to the interior of the continent (Fig. 3). However, it is worth noting in the Fujian province that these are coeval, but volumetrically major tholeiitic rocks in the Mingxi and Qingliu areas of Inner belt.

4. $^{40}Ar-^{39}Ar$ dating results

The $^{40}Ar/^{39}Ar$ dating results for 24 samples from the Zhejiang–Fujian area are plotted as age spectrum and $^{36}Ar/^{40}Ar-^{39}Ar/^{40}Ar$ isotope correlation diagrams in Figs. 4 and 5. A summary of the results is given in Table 3.

Fig. 4 shows the apparent age, Ca/K and Cl/K spectra, and the isotope correlation diagrams for two analyzed samples (Z6A and Z8) from Outer Middle belt of Zhejiang province. Both samples (Z6A and Z8) yield identical integrated dates of 10.4 ± 0.5 and 10.5 ± 0.5 Ma, respectively. The apparent dates for temperature steps >420 °C (Z6A) and >470 °C (Z8) are all consistent with each other within 2σ forming a perfect flat plateau over 95% of total gas released (Fig. 4), with plateau date of 10.4 ± 0.5 Ma for Z6A and 10.5 ± 0.5 Ma for Z8. Both plateau dates are all identical to their respective integrated dates. Nevertheless, there are some anomalously old dates appearing in the first few steps for both samples. The corresponding Ca/K and Cl/K ratios for these low temperature steps are also slightly higher than those of plateau steps. These anomalously old dates are most likely due to the outgassing of alteration phases, since alteration phases often exhibit higher Cl and Ca contents with respect to ordinary constitute minerals in volcanic rocks, as discussed by Lo et al. (1994). However, considering the facts that most of the plateau steps show consistent Ca/K and Cl/K ratios and that the gas fraction released from these discordant steps at low temperatures is relatively low (<5%) (Fig. 4), the possible effects of alteration in the present samples seem to be minor and can be negligible. Regression of the data for plateau steps in the $^{36}Ar/^{40}Ar-^{39}Ar/^{40}Ar$ correlation diagram indicates an intercept date of 10.1 ± 0.5 Ma, and a $^{40}Ar/^{36}Ar$ initial value of 297.4 ± 0.9, with the value of 0.77 for the mean sum of weighted deviate (MSWD), for Z6A. Whereas, Z8 sample yields an intercept date of 10.3 ± 0.5 Ma and a $^{40}Ar/^{36}Ar$ initial value of 296.8 ± 0.6, with an MSWD value of 1.05. These intercept date and the $^{40}Ar/^{36}Ar$ initial values are perfect in agreement with their corresponding plateau date and the atmospheric composition with $^{40}Ar/^{36}Ar$ ratio of 295.5, with MSWD values close to unity (Fig. 4). These would indicate that the K–Ar isotopic systematics in the samples has been kept in closed system since solidification, showing almost identical radiometric clocks in the samples.

Fig. 5 shows integrated and plateau dates, and age spectra for the other 22 samples analyzed. Similar to Z8 and Z6A, all the samples also display a fairly flat profile for the age spectra, exhibiting well-defined plateau over >68% of the total gas released, with some disturbed dates in the low- and high-temperature steps (Fig. 5). The disturbed steps usually exhibit Ca/K and Cl/K ratios distinct from those from the plateau steps, which may indicate the effects of outgassing from

Notes to Table 2:

[a] Rock types: QT, quartz tholeiite; OT, olivine tholeiite; AOB, alkali olivine basalt; B, basanite; N, nephelinite; APB, alkali picrite basalt.

[b] $\Sigma FeO = \Sigma Fe_2O_3/1.1$, and assuming that $Fe_2O_3 = 0.2$ FeO (Middlemost, 1989).

[c] MG (Mg-value) = 100 Mg/(Mg + Fe^{2+}).

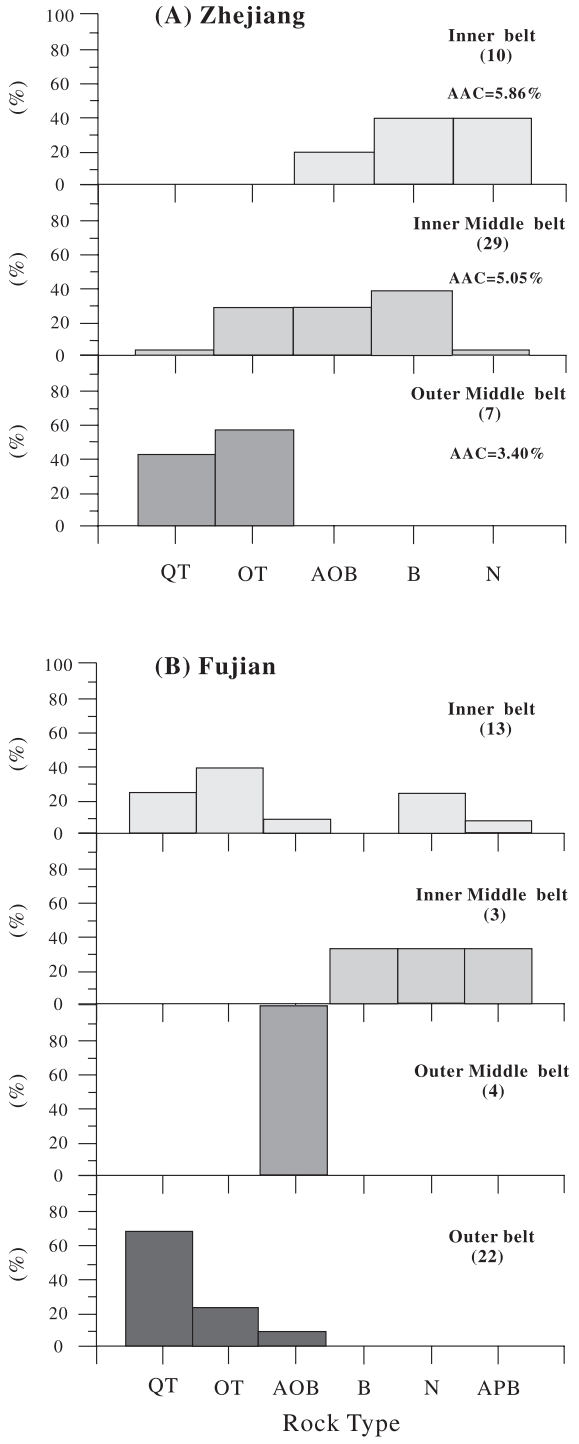

Fig. 3. Histogram showing distribution of basalt types for various volcanic belts in (A) Zhejiang and (B) Fujian Provinces. Numbers in longitudinal axis represent percentage of different rock types of the analyzed samples in each volcanic belt. Total amount of analyzed samples in each volcanic belt is labeled in parentheses. Analyzed data of the Inner Middle belt of Fujian after Sun and Lai (1980) and Liu et al. (1994). Abbreviations of rock types same as in Table 2. AAC: average of alkali contents.

alteration phases and some phenocrysts, similar to those described previously by Lo et al. (1994).

Regressions of plateau step data also suggest $^{40}Ar/^{36}Ar$ initial values in the range of 290.8–322.0, which are close to the atmospheric values, and intercept dates of 0.8–26.8 Ma, which are also concordant with their respective plateau dates in the range of 0.9–26.4 Ma, with statistically meaningful MSWD values of <2.83 (Table 3). All these perfectly meet the criteria of meaningful plateau dates, proposed by Lanphere and Dalrymple (1978), strongly indicating that all the obtained plateau dates can be considered as the best estimate for the ages of volcanic eruptions.

4.1. Zhejiang Segment

The oldest two samples dated are basanite Z31B from Longyou dike and nephelinite Z32A from Quzhou pipe in Inner belt, 26.4 ± 0.3 and 23.7 ± 0.3 Ma, respectively. Based on the stratigraphic relationships and relevant dating information of the Fujian Inner belt, the volcanic activity in the Quzhou region has previously been considered to be Pliocene by Liu et al. (1992). However, the present $^{40}Ar/^{39}Ar$ dating results show that the volcanic activity in this area may have taken place largely in early Miocene (Table 3). Volcanic breccia in the Jinyun area has entrained varied types of mantle xenoliths and megacrysts. The amphibole megacryst (17.0 ± 0.8 Ma) has similar radiometric age with the basanitic pipe (15.6 ± 0.7 Ma), suggesting that the amphibole megacryst may represent the product of earlier or simultaneous magmatic activities, and was captured during eruptive event.

The most extensive basaltic lava activity in the Zhejiang province is later than Jinyun basanitic pipe, Quzhou nephelinitic pipe and Longyou basanitic dike intrusion. The respective Ar–Ar ages of 10 basaltic lavas fall between 10.5 ± 0.5 and 2.5 ± 0.1 Ma. These results show that a magmatic quiescent period appears

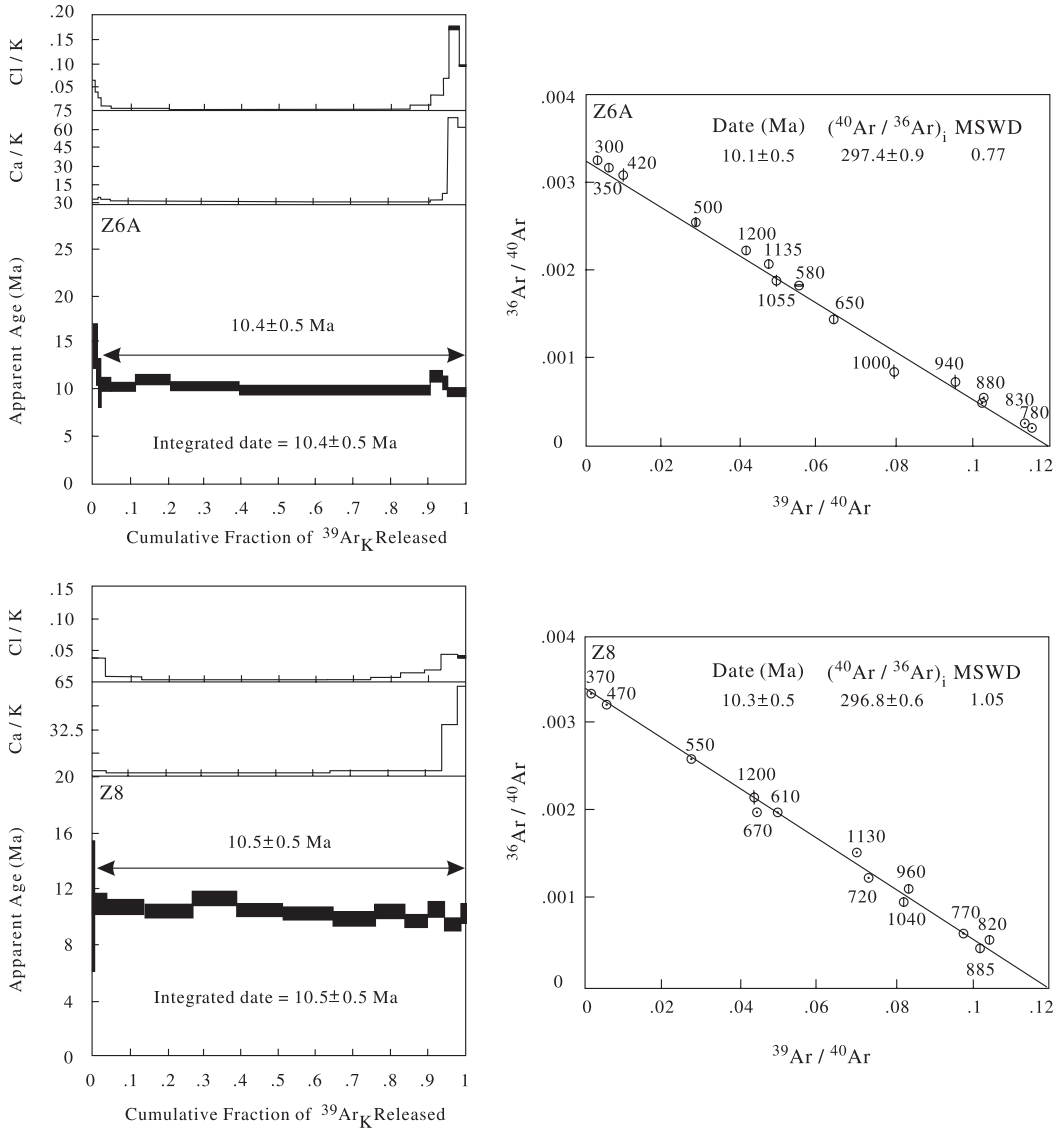

Fig. 4. Cl/K and Ca/K, and $^{40}Ar/^{39}Ar$ age spectra for two samples from Outer Middle belt, are shown on the left-hand side. The $^{36}Ar/^{40}Ar-^{39}Ar/^{40}Ar$ correlation diagrams and the regression results for these samples are shown on the right-hand side. In the spectrum plots, the bars represent $\pm 1\sigma$. All the errors are given in 1σ.

to have occurred from 15.6 to 10.5 Ma, and the magmatic activity was resumed at Shengxian–Xinchang region in the late Miocene. The Inner belt of Zhejiang is largely devoid of young volcanic activity except in the Zhuji area. The youngest age (2.5 ± 0.1 Ma) is registered in Z1A basanite from Zhuji lava, which may have recorded the latest volcanic activity in the Zhejiang province.

4.2. Fujian Segment

An alkali olivine basalt from Longhai, sample F24, exhibits a $^{40}Ar/^{39}Ar$ age of 15.7 ± 0.6 Ma. Four tholeiites from the Outer belt yield ages from 17.1 ± 0.6 to 14.8 ± 0.6 Ma (Table 3). It is clear that no obvious relationship exists between the eruptive age and rock type for the Outer belt basalts.

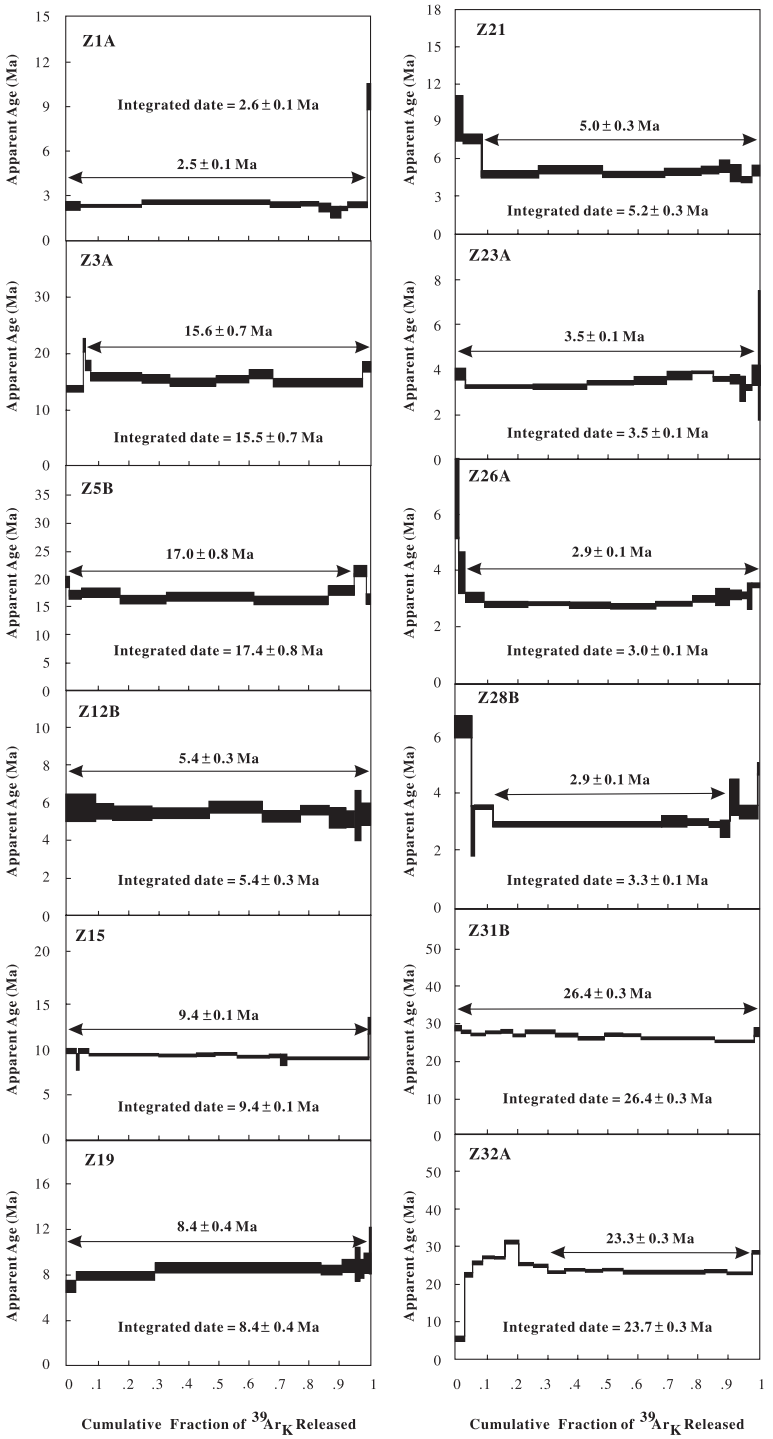

Fig. 5. Age spectra, integrated and plateau dates for 22 samples studied.

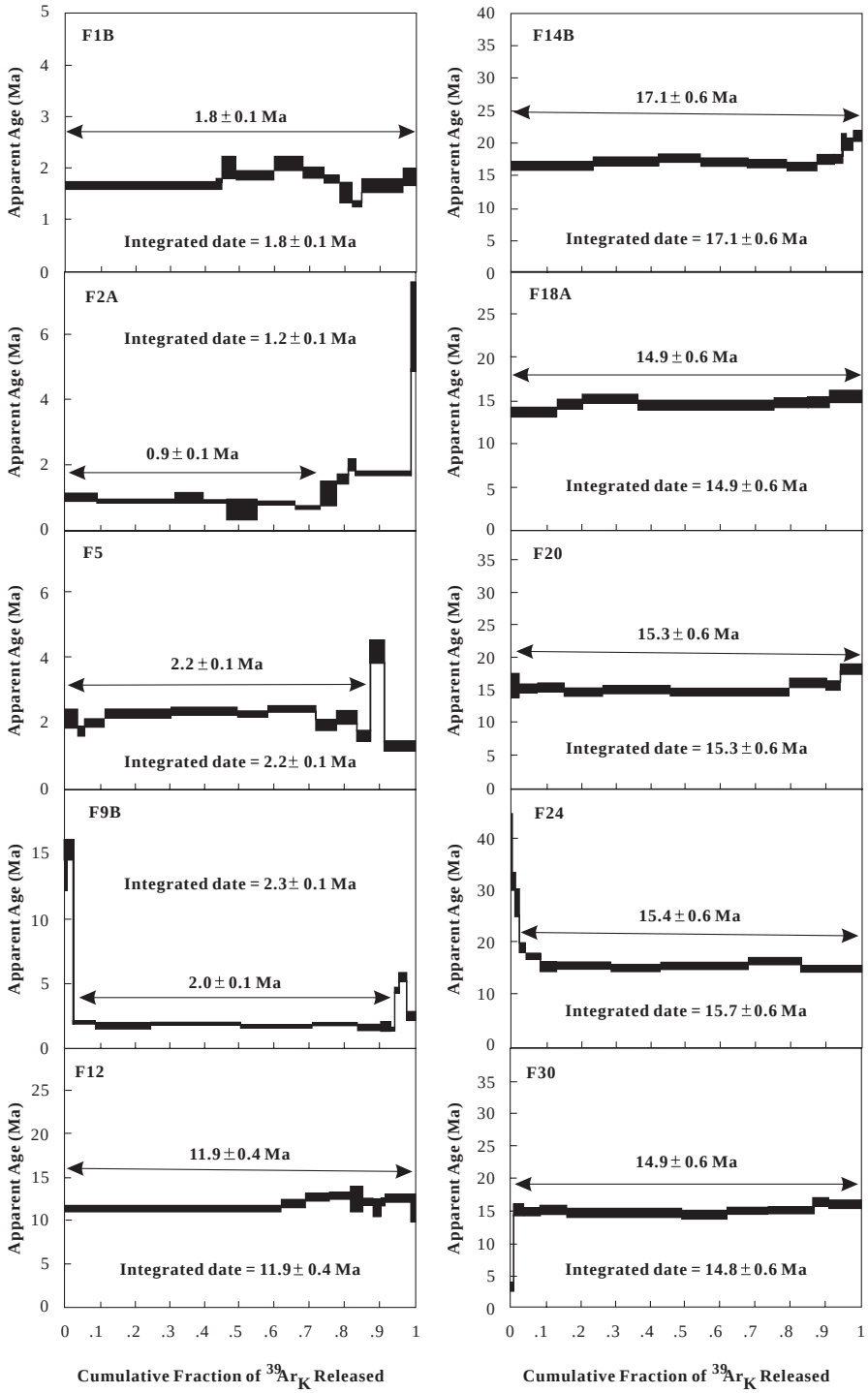

Fig. 5 (*continued*).

Table 3
Summary of $^{40}Ar/^{39}Ar$ dating results for the basaltic rocks and an amphibole megacryst from Zhejiang–Fujian area

Sample no.	Rock/mineral[a]	Occurrence	Locality	Integrated date[b] (Ma)	Plateau date[b] (Ma)	Intercept date[b] (Ma)	$(^{40}Ar/^{36}Ar)_i$[c]	MSWD
Zhejiang—Inner belt								
Z-1A	B	Lava	Zhuji	2.6 ± 0.1	2.5 ± 0.1	2.4 ± 0.1	295.6 ± 11.0	0.59
Z-32A	N	Pipe	Quzhou	23.7 ± 0.3	23.3 ± 0.3	23.4 ± 0.3	290.8 ± 5.0	1.83
Z-31B	B	Dike	Longyou	26.4 ± 0.3	26.4 ± 0.3	26.8 ± 0.3	303.4 ± 1.9	1.09
Zhejiang—Inner Middle belt								
Z-26A	AOB	Lava	Shengxian	3.0 ± 0.1	2.9 ± 0.1	2.9 ± 0.2	298.5 ± 0.3	1.18
Z-28B	AOB	Lava	Shengxian	3.3 ± 0.1	2.9 ± 0.1	2.9 ± 0.1	309.0 ± 1.0	0.77
Z-23A	OT	Lava	Shengxian	3.5 ± 0.1	3.5 ± 0.1	3.6 ± 0.1	298.4 ± 0.5	0.17
Z-21	AOB	Lava	Xinchang	5.2 ± 0.3	4.9 ± 0.3	4.9 ± 0.3	302.7 ± 0.2	0.41
Z-12B	B	Lava	Tiantai	5.4 ± 0.3	5.4 ± 0.3	5.4 ± 0.3	295.0 ± 1.0	0.48
Z-19	OT	Lava	Xinchang	8.4 ± 0.4	8.4 ± 0.4	8.5 ± 0.4	303.7 ± 6.5	0.69
Z-15	B	Lava	Xinchang	9.4 ± 0.1	9.4 ± 0.1	9.4 ± 0.1	299.9 ± 4.2	2.64
Z-3A	B	Pipe	Jinyun	15.5 ± 0.7	15.6 ± 0.7	15.6 ± 0.7	305.5 ± 7.7	2.83
Z-5B	Amphi	Meg.	Jinyun	17.4 ± 0.8	17.0 ± 0.8	17.0 ± 0.1	299.0 ± 0.3	0.38
Zhejiang—Outer Middle belt								
Z-6A	OT	Lava	Linhai	10.4 ± 0.5	10.4 ± 0.5	10.1 ± 0.5	297.4 ± 0.9	0.77
Z-8	OT	Lava	Ninghai	10.5 ± 0.5	10.5 ± 0.5	10.3 ± 0.5	296.8 ± 0.6	1.05
Fujian—Inner belt								
F-2A	N	Lava	Mingxi	1.2 ± 0.1	0.9 ± 0.1	0.8 ± 0.1	321.1 ± 1.4	0.36
F-1B	N	Lava	Mingxi	1.8 ± 0.1	1.8 ± 0.1	1.8 ± 0.1	295.1 ± 4.4	1.73
F-5	AOB	Lava	Mingxi	2.2 ± 0.1	2.2 ± 0.1	2.4 ± 0.1	295.5 ± 8.0	2.79
F-9B	OT	Lava	Qingliu	2.3 ± 0.1	2.0 ± 0.1	1.9 ± 0.3	305.9 ± 1.1	0.29
Fujian—Outer Middle belt								
F-12	AOB	Lava	Minqing	11.9 ± 0.4	11.9 ± 0.4	12.5 ± 0.5	294.7 ± 4.0	2.34
Fujian—Outer belt								
F-30	OT	Lava	Zhangpu	14.8 ± 0.6	14.9 ± 0.6	14.7 ± 0.6	298.2 ± 7.5	2.68
F-18A	OT	Lava	Longhai	14.9 ± 0.6	14.9 ± 0.6	15.3 ± 0.6	308.3 ± 2.7	0.47
F-20	OT	Lava	Longhai	15.3 ± 0.6	15.3 ± 0.6	15.0 ± 0.6	317.0 ± 10.3	1.87
F-24	AOB	Lava	Longhai	15.7 ± 0.6	15.4 ± 0.6	15.4 ± 0.6	302.1 ± 9.6	1.14
F-14B	QT	Lava	Longhai	17.1 ± 0.6	17.1 ± 0.6	17.1 ± 0.6	322.0 ± 3.4	1.54

[a] Abbreviations of rock types same as in Table 1. Amphi: amphibole.
[b] All age errors are shown in 1σ.
[c] $(^{40}Ar/^{36}Ar)_i$ values were obtained from the regression of the plateau steps on isotope correlation diagram.

The plateau age of an Outer Middle belt alkali olivine basalt yields 11.9 ± 0.4 Ma, which is younger than the previous conclusion of 14.1 ± 0.3 Ma by Liu et al. (1992) deduced from K–Ar dating method.

$^{40}Ar/^{39}Ar$ dating of one olivine tholeiite, one alkali olivine basalt, and two nephelinites from the Inner belt suggests ages ranging from 0.9 ± 0.1 to 2.2 ± 0.1 Ma. These ages are generally concordant with the younger ages (0.7 ± 0.1–3.0 ± 0.1 Ma) measured previously by K–Ar method (Liu et al., 1992). However, the K–Ar ages of two basanites and one limburgite, ranging from 4.5 ± 0.1 to 5.0 ± 0.2 Ma (Liu et al., 1992), appear to be older than the Ar–Ar ages obtained by this study. Without information for the samples dated by Liu et al. (1992), it is difficult to further interpret the discrepancies. Given that the present samples are fresh and that all the plateau dates are considered to be meaningful as discussed earlier, the $^{40}Ar/^{39}Ar$ ages presented in the study should be reliable.

In summary, $^{40}Ar-^{39}Ar$ dating of 10 samples in the Fujian province yields eruption ages ranging from 17.1 to 0.9 Ma (Table 3), corresponding to middle Miocene to late Pleistocene. The eruption ages, 17.1–14.8, 11.9 and 2.2–0.9 Ma, indicate that there are three periodic volcanic eruptions, migrating from east to west with geological time, and the first stage magmatism is the most voluminous.

5. Bulk chemistry

5.1. Major and trace elements

The abundance of major and trace (including the rare earths) elements of the representative basaltic rocks in Zhejiang–Fujian area are listed in Table 2. The analyzed samples show wide range in chemistry

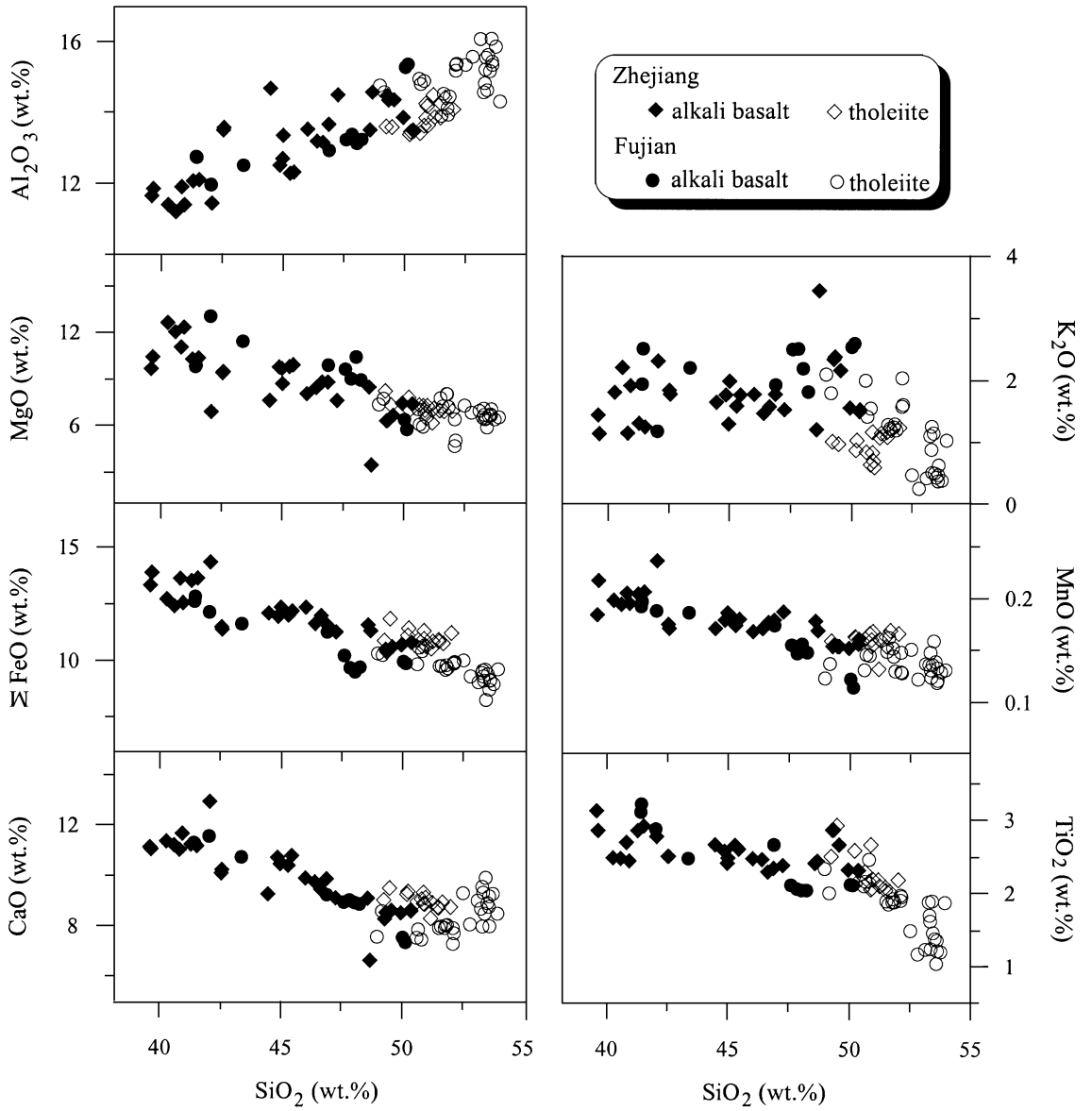

Fig. 6. Major element vs. SiO_2 plots for basalts from the Zhejiang–Fujian area.

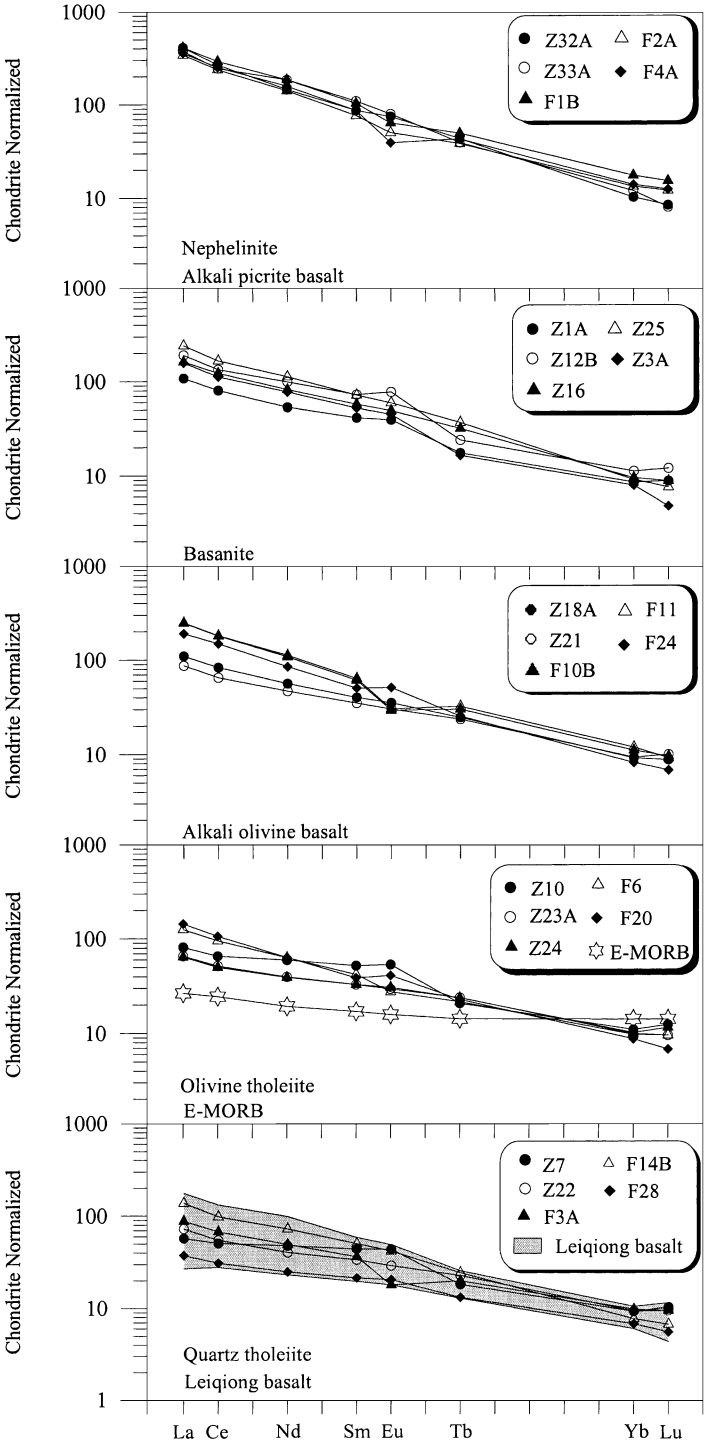

Fig. 7. Chondrite-normalized REE distribution of representative basaltic rocks from Zhejiang–Fujian area. Note that the samples show strong LREE-enriched patterns with $(La/Yb)_N = 4.9$ to 42.9. REE ranges of Leiqiong basalts are from Ho et al. (2000a); E-MORB data and the normalizing values are from Sun and McDonough (1989).

and vary from strongly undersaturated nephelinites and alkali picrite basalts through mildly undersaturated basanites and alkali olivine basalts to olivine tholeiites and quartz tholeiites. All analyzed samples have SiO_2 ranging from 39.57% to 53.92%. The silica contents are generally good indicators of different basaltic suites. Most of the tholeiitic rocks have higher SiO_2 contents than the alkali suites.

In Zhejiang–Fujian area, only a few nephelinites (e.g., Z32A, F2A) have Mg-values (100 Mg/(Mg + Fe^{+2})) between 68.4 and 68.9, MgO 11.45–12.65%, Ni 306–379 ppm and Cr 326–405 ppm which match the composition of primary basalt defined by Hart and Allegre (1980). Most of the basaltic rocks have low Mg-values, and low and varied concentrations of MgO, Ni and Cr indicate that they may not represent primitive basalts and probably have undergone certain degree of fractional crystallization. Based on the systematic increase of Al_2O_3, and decrease of ΣFeO, MgO, CaO and MnO with increasing SiO_2 contents (Fig. 6), the Zhejiang–Fujian basalts may have experienced fractional crystallization of ferromagnesian minerals such as olivine and clinopyroxene after the formation of the initial liquid. In addition, the abundances of K_2O and TiO_2 are negatively correlated with SiO_2 contents of the Fujian tholeiites (Fig. 6). It is suggested that fractional crystallization of feldspar and Ti-bearing opaques may have occurred during magmatic evolution.

The total alkali contents ($Na_2O + K_2O$) of the basaltic rocks from Zhejiang–Fujian area are always higher than 2.5%, and the Na_2O/K_2O ratios of all basalts studied are more than unity indicating their alkali-enriched and high-sodium nature. However, the Na_2O content in alkali picrite basalt (F4A) is around 1.34%, which is lower than those in the other rock types ($Na_2O = 2.25–5.03\%$). Alkali picrite basalt has high-Mg and low alkali contents which correspond to picrobasalt of IUGS classification system (Le Bas, 2000).

The chondrite-normalized rare earth element (REE) patterns of basaltic rocks from Zhejiang–Fujian area show moderate to steep sloping with light rare earth element (LREE) enrichment (Fig. 7). The $(La/Yb)_N$ ratios increase with the undersaturated character from 4.9 to 17.7 in the quartz tholeiites, 6.0 to 25.6 in the olivine tholeiites, 9.5 to 35.0 in the alkali olivine basalts, 12.2 to 27.0 in the basanites, and 23.6 to 42.9 in the nephelinites and alkali picrite basalt. The LREE abundance in tholeiitic basalts is higher than that of E-type mid-ocean ridge basalts (Sun and McDonough, 1989), but is comparable with Leiqiong basalts (Ho et al., 2000a) (Fig. 7).

5.2. Sr–Nd isotopic composition

Basaltic rocks of Zhejiang–Fujian area show a wide range of isotopic composition with $^{87}Sr/^{86}Sr = 0.703264–0.704235$ and $^{143}Nd/^{144}Nd = 0.512725–0.512961$ (Table 4). These results are similar to the Sr and Nd isotopic compositions of the Leiqiong basalts ($^{87}Sr/^{86}Sr = 0.703101–0.704624$; $^{143}Nd/$

Table 4
Sr–Nd isotopic compositions of late Cenozoic basaltic rocks in the Zhejiang–Fujian area

Volcanic belt	Sample no.	Locality	Rock type[a]	$^{87}Sr/^{86}Sr$[b]	$^{143}Nd/^{144}Nd$[b]	εNd[c]
Outer Middle belt	F12	Minqing	AOB	0.703833 ± 8	0.512845 ± 18	+4.0
	Z6A	Linhai	OT	0.703264 ± 9	0.512961 ± 13	+6.3
	Z11B	Ninghai	QT	0.704140 ± 12	0.512892 ± 9	+5.0
Inner Middle belt	Z5A	Jinyun	N	0.703557 ± 7	0.512890 ± 16	+4.9
	Z12B	Tiantai	B	0.703678 ± 10	0.512902 ± 9	+5.2
	Z26A	Shengxian	AOB	0.703736 ± 9	0.512910 ± 11	+5.3
	Z24	Shengxian	OT	0.704235 ± 11	0.512873 ± 10	+4.6
	Z22	Xinchang	QT	0.704189 ± 7	0.512725 ± 26	+1.7
Inner belt	Z32A	Quzhou	N	0.703704 ± 7	0.512864 ± 6	+4.4
	Z31B	Longyou	B	0.703817 ± 8	0.512875 ± 17	+4.6
	Z1C	Zhuji	AOB	0.703885 ± 10	0.512915 ± 9	+5.4

[a] Abbreviations of rock types same as in Table 1.
[b] Errors of $^{87}Sr/^{86}Sr$ and $^{143}Nd/^{144}Nd$ are shown in 2σ.
[c] $\varepsilon Nd = ((^{143}Nd/^{144}Nd)_{sample}/(^{143}Nd/^{144}Nd)_{CHUR}) - 1) \times 10^4$ $(^{143}Nd/^{144}Nd)^{0Ma}_{CHUR} = 0.512638$.

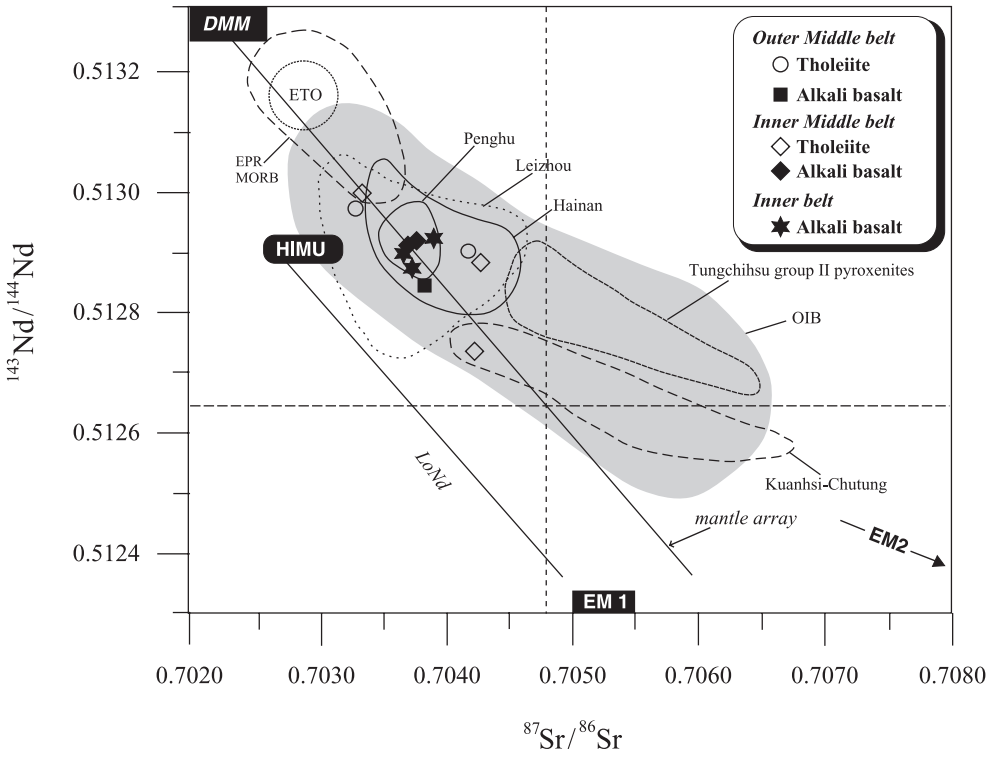

Fig. 8. Plots of $^{143}Nd/^{144}Nd$ vs. $^{87}Sr/^{86}Sr$ diagram for the Zhejiang–Fujian basalts. The fields for the Tungchihsu group II pyroxenites (Ho et al., 2000b), and the late Cenozoic basalts of Leizhou, Hainan, Penghu, and Kuanhsi–Chutung (NW Taiwan) regions (Peng et al., 1986; Zhu and Wang, 1989; Zhao, 1990; Basu et al., 1991; Tu et al., 1991; Zhang and Chen, 1992; Lan et al., 1994; Lee, 1994; Chung et al., 1995) are shown for comparison. The fields of DMM, HIMU, EM1 and EM 2 are from Zindler and Hart (1986); the East Taiwan Ophiolite (ETO) N-type basalts field is from Jahn (1986) and Chung and Sun (1992); the East Pacific Rise (EPR) MORB field is from Wilson (1989); the OIB field is from Staudigel et al. (1984). LoNd = Low Nd array (Hart et al., 1986).

$^{144}Nd = 0.512736–0.513039$, Zhu and Wang, 1989; Zhao, 1990; Tu et al., 1991). On the $^{143}Nd/^{144}Nd$ vs. $^{87}Sr/^{86}Sr$ diagram (Fig. 8), the Zhejiang–Fujian basalts plot within the OIB field and most of samples are closely related to the mantle array.

6. Discussion

6.1. Geochemical characteristics of the Zhejiang–Fujian basaltic rocks and implications for their mantle sources

The Zr/Nb ratios of the Zhejiang–Fujian basaltic rocks analyzed vary from 2.0 to 10.7, and the Zr/Y ratios vary from 5.0 to 16.2. These incompatible element ratios of basaltic rocks are higher than those of MORB, but are similar to those observed in ocean island basalts (average Zr/Nb and Zr/Y ratios of OIB are 5.8 and 9.7, respectively, Sun and McDonough, 1989). In general, LREE are highly incompatible in the mantle–melt system, the LREE ratios should be close to those of the mantle source under a batch melting condition (Sun and Hanson, 1975). The La/Ce (0.44–0.65) and Ce/Sm (4.6–12.6) ratios of the Zhejiang–Fujian basaltic rocks appear to be higher than those of primitive mantle (0.39 and 4.0, respectively, Sun and McDonough, 1989), strongly reflecting their derivation from a fertile mantle source.

In chondrite-normalized REE patterns (Fig. 7), except exhibiting strong LREE enrichment, a few basaltic rocks also have slightly positive or negative Eu anomalies. Philpotts and Schnetzler (1968) suggested that fractional crystallization of 18% or more

plagioclase from the magma could cause 5% or more negative Eu anomaly in the basaltic rocks. Therefore, the analyzed samples such as F3A, F10B and F11 have REE spectra with slightly negative Eu anomalies, which can be attributed to the fractionation of plagioclase playing an important role during the generation and evolution of these magmas. On the other hand, the Eu enrichment of the basaltic rocks (e.g., Z1A, Z7, Z10, Z12B, F20, F24) can be considered as the result of a natural consequence of partial melting of the mantle under reducing conditions (Sun and Hanson, 1975). In addition, the plagioclase megacrysts in basaltic rocks have been found in some localities such as at Xinchang and Longhai (Chih, 1988), if the early crystallized plagioclase megacrysts mixed into the magma source, it could also produce a positive Eu anomaly in the melt.

The primitive mantle-normalized incompatible element diagrams of Zhejiang–Fujian basalts are quite similar to that of the average oceanic island basalts, although a few alkali basalts show Ba and K "troughs" and Li "peak" (Fig. 9). The nephelinite and alkali picrite basalt have slight negative K anomalies, but their Ba/Rb ratios (except Z33A sample) are similar to those of the intraplate basalts (~ 12, Sun and McDonough, 1989), which may be interpreted as due to K-bearing minerals in the residual phases. In general, if degree of partial melting of mantle source increased, then the percentage of partial melting of K-bearing minerals in the mantle source will also increase. Therefore, the tholeiitic basalts, which have lower incompatible element contents than the alkali basalts and show no distinct negative K anomalies, may have been derived from larger degree of partial melting. It is suggested that the incompatible elements such as LREEs contents generally increase with decreasing SiO_2 saturation (Fig. 7). These regular compositional variations may reflect the chemical characteristics and different degree of partial melting of a garnet- or spinel-lherzolite mantle source. Therefore, it is believed that the quartz tholeiite or olivine tholeiite were derived from relative shallow mantle source through a larger degree of partial melting, while the alkali basalts were formed from deeper mantle source through a smaller degree of partial melting.

Unlike other late Cenozoic intraplate basalts in SE China, the alkali-rich nephelinite and magnesium-rich alkali picrite basalt have been found in the Inner and Inner Middle belts in Zhejiang–Fujian region. Analyses of five nephelinite samples in this study show that they have restricted incompatible compositions and are strongly enriched in Hf, Sr, Th and LREEs typical of alkaline rocks (Table 2). However, sample Z33A has abundant clinopyroxene, analcite and rare olivine, titano-magnetite, with a lower chrome content (208 ppm) and Mg-value (61.8) which is similar to the melanephelinite found on the western Kenya area, Africa (Le Bas, 1987). The most striking chemical feature of melanephelinite is the strong depletion in barium (Ba = 77 ppm) and the enrichment in lithium (Li = 110 ppm) relative to those found in the nephelinites (Ba = 671–1068 ppm; Li = 9–23 ppm) (Fig. 9). It should be noted that the melanephelinite dike hosts numerous Ti-mica megacrysts, which contain very high amount of barium (Ba = 734 ppm, Ho, 1999). The Ti-mica megacrysts belonging to Group B (Irving, 1984) were considered to be xenocrysts derived from a relatively evolved magma, and were brought up to the earth's surface by ascending basaltic magma at a later stage. According to the experiment of LaTourrette et al. (1995), the barium and lithium partition coefficients between mica and basaltic melt under mantle condition are 3.68 and 0.064, respectively. Crystallization of large amounts of mica from the parental magma may therefore affect the barium and lithium signatures in the residual magma (Ho, 1999).

6.2. Petrogenesis of the late Cenozoic Zhejiang–Fujian basalts

6.2.1. Mantle metasomatism beneath SE China

Alkali basalts in SE China contain varied amounts of mantle xenoliths and high-pressure megacrysts that can provide a good opportunity to reveal chemical compositions and processes in the lithospheric mantle. Detailed petrographic and geochemical investigations (Fan and Hooper, 1989; Qi et al., 1995; Ho et al., 2000b) showed that the lithospheric mantle beneath the SE China is compositionally and isotopically heterogeneous, reflecting possible experience of depletion and enrichment events.

In general, the metasomatically enriched xenoliths are characterized by hydrous and other exotic accessory phases. In SE China, amphibole and phlogopite megacrysts were found in Jinyun and Quzhou, Zhe-

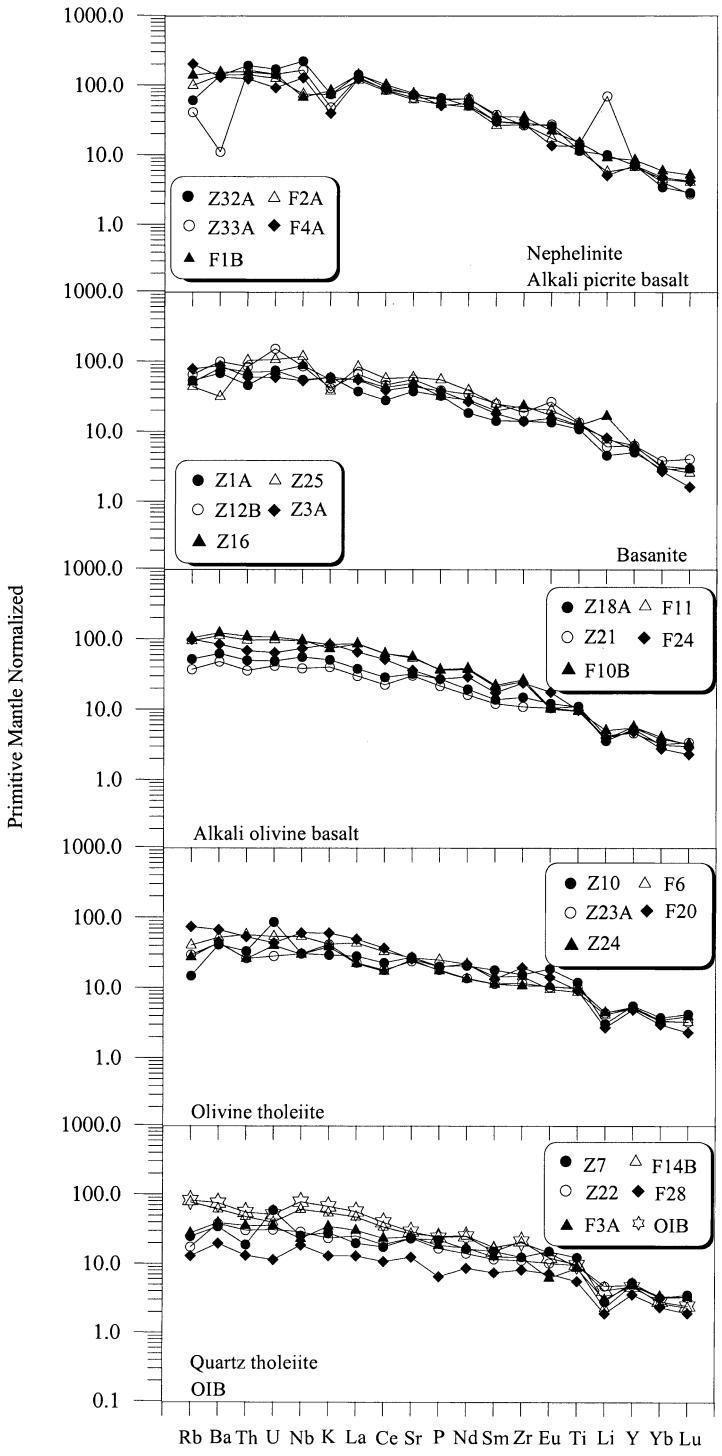

Fig. 9. Primitive mantle-normalized incompatible element patterns for selected basaltic rocks from Zhejiang–Fujian area. Note that the samples are enriched in highly incompatible trace elements similar to those of OIB. OIB data and the normalizing values are from Sun and McDonough (1989).

jiang province and Tungchihsu, Penghu Islands in the Taiwan Strait. In addition, some mantle lherzolites, pyroxenites and composite xenoliths in Mingxi, Fujian province; Puning, Guangdong province and Tungchihsu of Penghu Islands contain certain amount of amphibole or mica, commonly interstitial and secondary in origin (Zhao, 1990; Ho et al., 2000b; and unpublished data). These evidences show that the depleted lithospheric mantle beneath SE China was affected by metasomatism.

Late Cenozoic basalts in Zhejiang–Fujian, Leiqiong area and South China Sea Basin have high $^{208}Pb/^{204}Pb$ (37.610–39.260) and $^{207}Pb/^{204}Pb$ (15.437–15.649) ratios which plot above the Northern Hemisphere Reference Line indicating Dupal anomaly toward EM2 direction (Peng et al., 1986; Zhu and Wang, 1989; Basu et al., 1991; Tu et al., 1991, 1992; Lan et al., 1994; Zou et al., 2000). It is generally believed that the EM2 component of the basalts may be derived from continental lithospheric mantle such as Tungchihsu group II pyroxenitic rocks (Fig. 8). Chung et al. (1994) suggested that the EM2 component of continental lithospheric mantle is related to the subduction of the Pacific plate beneath the Eurasian plate in Mesozoic. Zhang et al. (1996) also concluded that the mantle source of Leiqiong basalts might have been affected by sediments associated with a paleo-subduction zone. The negative Nb anomaly observed in the spidergram of some basalts (Fig. 9) indicated that the influence of a paleo-subduction zone derived component could not be excluded in considering the genesis of the basalts from the Zhejiang–Fujian area.

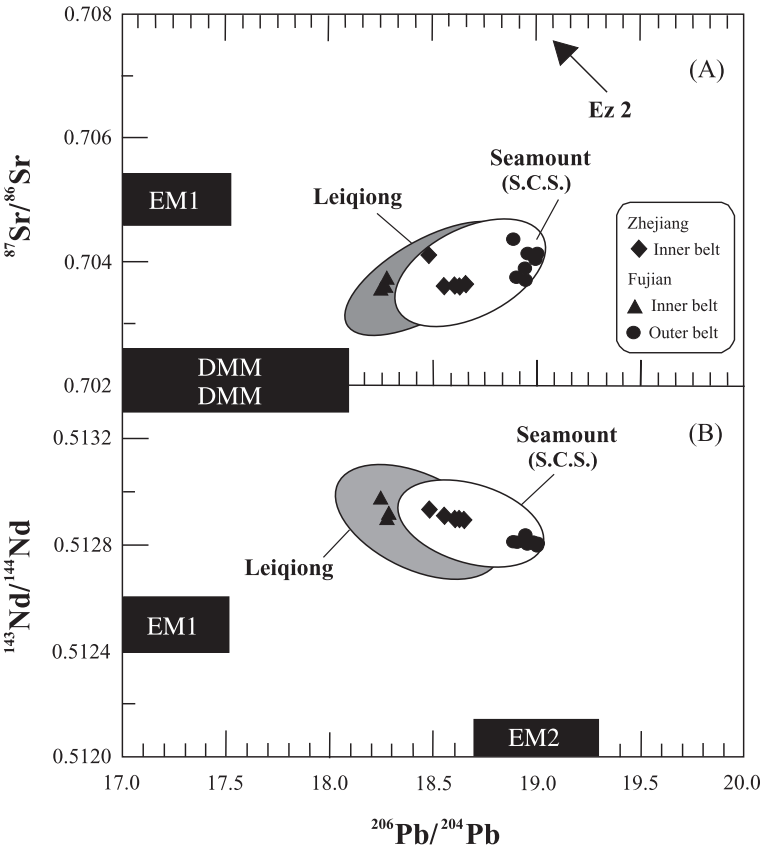

Fig. 10. $^{87}Sr/^{86}Sr$ vs. $^{206}Pb/^{204}Pb$ and $^{143}Nd/^{144}Nd$ vs. $^{206}Pb/^{204}Pb$ diagrams for the Zhejiang–Fujian basalts. The fields for the Leiqiong (Zhu and Wang, 1989; Tu et al., 1991) and South China Sea seamount (Tu et al., 1992) are shown for comparison. The fields of DMM, EM1 and EM2 are adopted from Zindler and Hart (1986). Sr, Nd and Pb isotope compositions of Zhejiang–Fujian basalts are from Peng et al. (1986), Basu et al. (1991), Lan et al. (1994) and Zou et al. (2000).

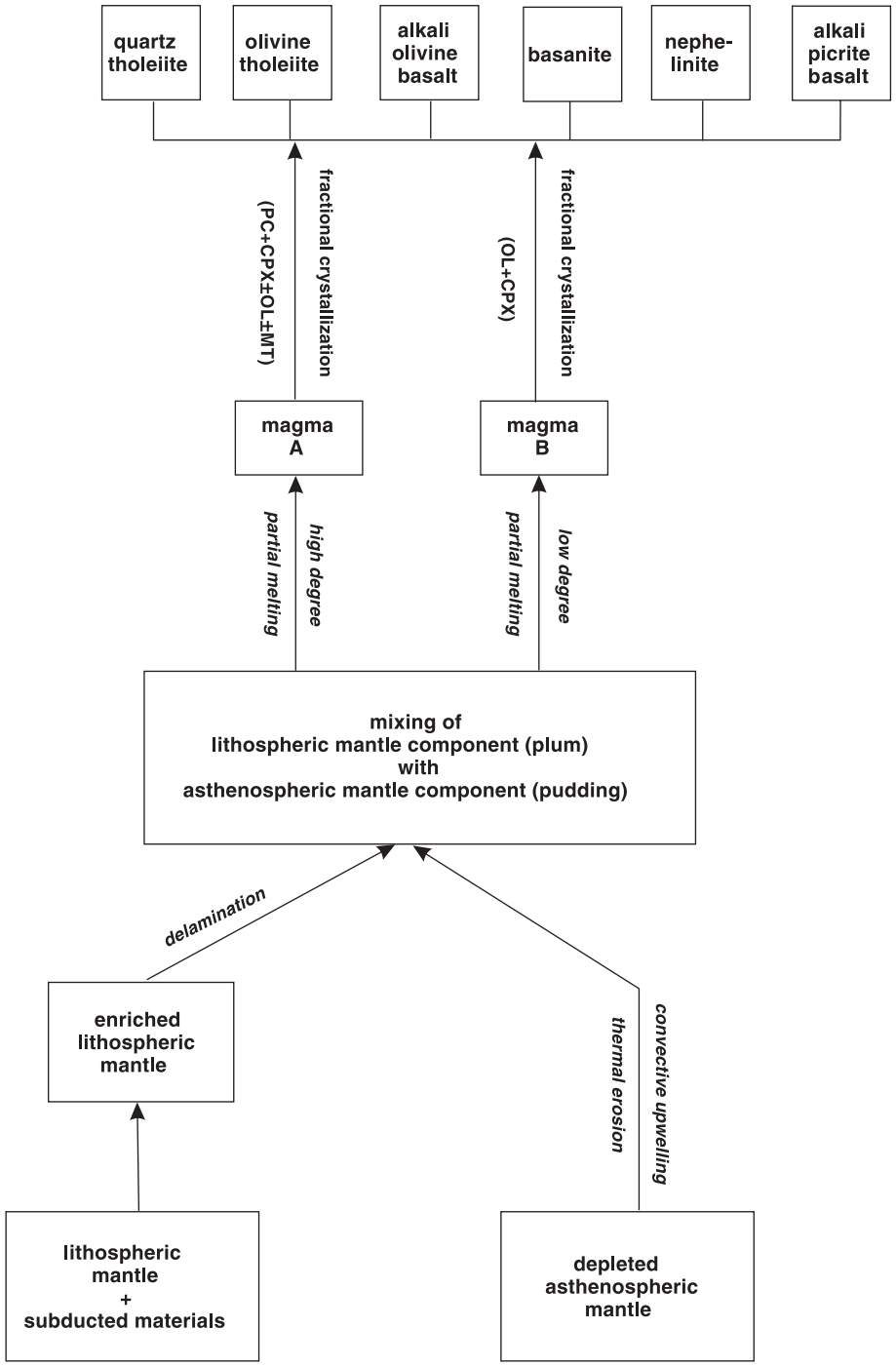

Fig. 11. A petrogenetic model for the late Cenozoic basaltic rocks from Zhejiang–Fujian region, SE China. Abbreviation: PC: plagioclase; OL: olivine; CPX: clinopyroxene; MT: Ti–Fe oxide minerals.

6.2.2. The isotopic characteristics and generation of basalts

Sr, Nd and Pb isotope compositions of Zhejiang–Fujian basalts were presented by Peng et al. (1986), Zhao (1990), Basu et al. (1991), Zhang and Chen (1992), Lan et al. (1994), Zou et al. (2000) and this study. Limited isotopic data have shown spatial chemical and isotopic variations in the basalts. In the Zhejiang province, except one olivine tholeiite Z6A, tholeiitic basalts have higher $^{87}Sr/^{86}Sr$ (0.704140–0.704235) and lower $^{143}Nd/^{144}Nd$ (0.512725–0.512932) ratios than those of alkali basalts which have $^{87}Sr/^{86}Sr$ ranging from 0.703292 to 0.703885 and $^{143}Nd/^{144}Nd$ ranging from 0.512864 to 0.512990. In the Fujian province, except Inner belt, tholeiite has a wide Sr isotope range, in general $^{87}Sr/^{86}Sr$ and $^{206}Pb/^{204}Pb$ ratios of the basalt increase progressively from the Inner to the Outer belts. In addition, Sr and Nd isotopic compositions of Outer belt alkali basalts overlap with those of tholeiites.

In $^{143}Nd/^{144}Nd$ vs. $^{206}Pb/^{204}Pb$ and $^{87}Sr/^{86}Sr$ vs. $^{206}Pb/^{204}Pb$ diagrams (Fig. 10), the plots show that the Zhejiang–Fujian basalts can be produced by DMM (depleted MORB mantle) and EM2 (enriched mantle with high $^{206}Pb/^{204}Pb$, high $^{87}Sr/^{86}Sr$ and intermediate $^{143}Nd/^{144}Nd$, Zindler and Hart, 1986) components mixing. Based on the genetic model proposed by Chung et al. (1994), the SE China lithosphere thinning occurred during the Miocene and that the lithospheric mantle was thermomechanically eroded by convective upwelling of the asthenosphere, and created a plum-pudding type convecting mantle domain. Therefore, the spatial chemical and isotopic variation in the Zhejiang–Fujian basalts can be explained by different degrees of decompression melting of the convecting mantle compounded by variable contributions from the continental lithospheric mantle (CLM)-derived plume (i.e., enriched) component. The voluminous tholeiites in the Outer belt owe their generation largely to lithospheric mantle which has undergone extensive melting near the locus of upwelling.

The Sr–Nd isotope geochemistry of Zhejiang–Fujian and other SE China basalts showed that some basalts exhibit considerable deviation from the MORB-OIB array (Fig. 8), a feature which may be accounted for by involving Tungchihsu group II pyroxenite components (with high $^{87}Sr/^{86}Sr$) in the magma evolution. We suggest that the SE China basalts were produced through mixing of various proportions of two mantle components. The depleted asthenosphere component is represented by the East Taiwan Ophiolite (ETO) N-type basalt (Chung et al., 1994; Lan et al., 1994), while the enriched lithosphere component is partly represented by the Tungchihsu group II pyroxenite.

A simple petrogenetic model for late Cenozoic Zhejiang–Fujian basaltic rocks is sketched in Fig. 11. In general, the mantle source of tholeiitic magma may have mixed with a more enriched component and undergone a relatively higher degree of partial melting than that of the alkali basalt magma. In addition, low-pressure fractionation has also occurred in Zhejiang–Fujian basaltic magma. Based on major and trace elements studies, the alkali basalts have mainly fractionated olivine and clinopyroxene, while the tholeiitic basalts have fractionated plagioclase, clinopyroxene and/or minor amounts of Fe–Ti oxide minerals and olivine.

6.3. Late Cenozoic volcanic activities in the Zhejiang–Fijian area: eruption ages and tectonic implications

In the Zhejiang–Fujian area, sparse volcanic activities occurred and produced small amounts of basanite dikes and nephelinite pipes in the Zhejiang Inner

Fig. 12. Sketch map of South China Sea and adjacent areas exhibiting spatial and temporal distribution of late Cenozoic intraplate basaltic flows and major tectonic features. Solid lines in Zhejiang–Fujian–Guangdong area represent four volcanic belts as labeled in Fig. 1. Marine magnetic anomalies in the South China Sea after Taylor and Hayes (1983) and Briais et al. (1993). Identified marine magnetic anomalies are indicated by Anomaly number. Hatched lines depict the boundary of oceanic crust and double dashed lines represent inactive spreading centers. Arrows indicate the direction of thermal center migration since the beginning of mid-Miocene as discussed in the text. Radiometric ages, given in Ma, for late Cenozoic basalts from Zhejiang–Fujian area are compiled from Wang and Yang (1987), Liu et al. (1992) and this study. For Penghu Islands and NW Taiwan, the data are from Chen (1990), Juang and Chen (1992), Lee (1994) and Juang (1996). For Leizhou Peninsula and Hainan Island, the data are from Zhu and Wang (1989), Ge et al. (1989), Sun (1991) and Ho et al. (2000a). For Indochina Peninsula, the data are from Barr and MacDonald (1981), Arvanne et al. (1990), Rangin et al. (1995) and Lee et al. (1998).

volcanic belt before cessation of the South China Sea floor spreading. By comparison, the eruption process was comparatively active after cessation of the spreading of the South China Sea, and a large amount of basaltic lavas with minor pyroclastic rocks erupted to form a diffuse volcanic province (Fig. 12).

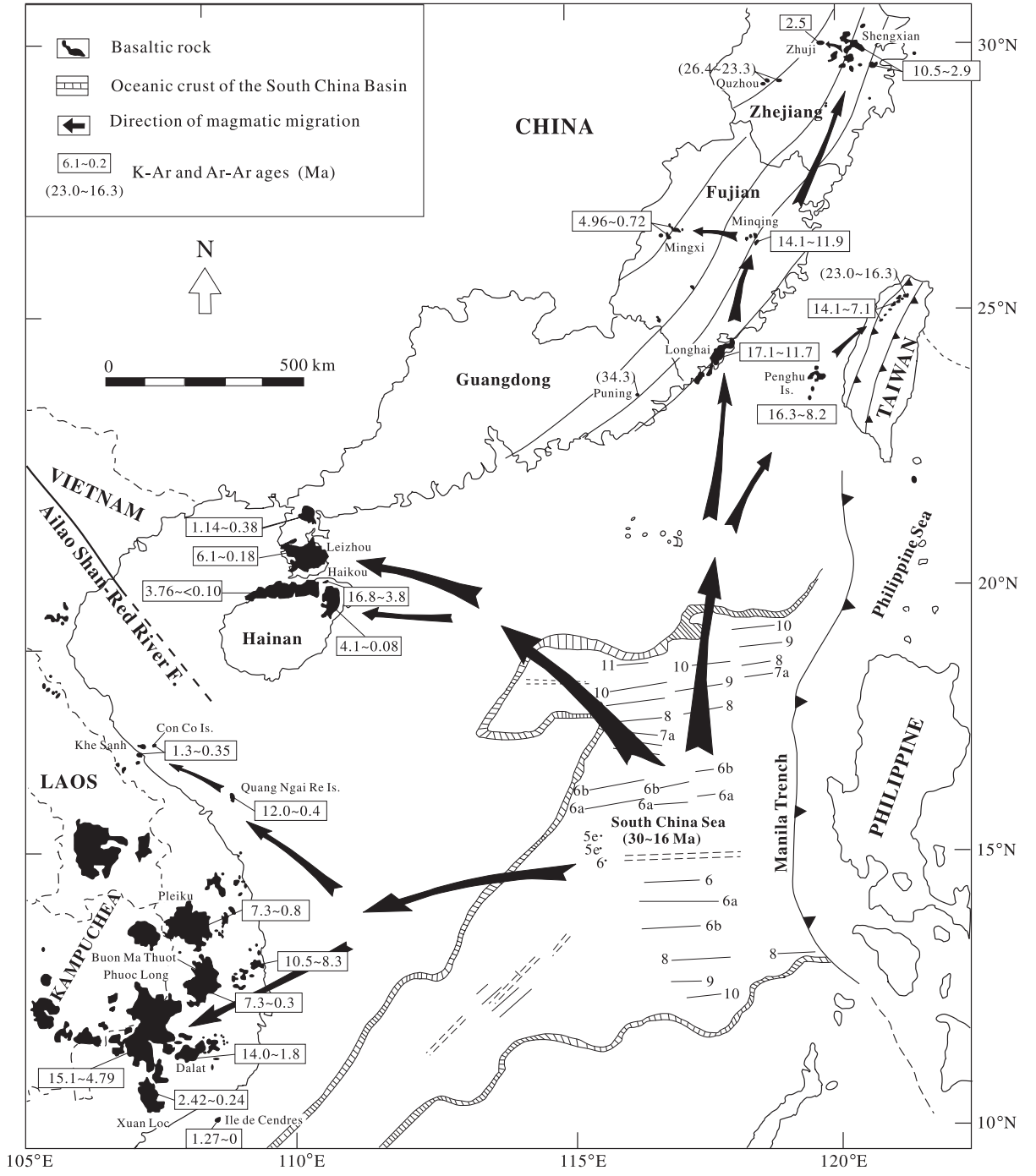

The timing of the initial volcanic eruptions in Fujian Outer belt is still under debate. Some of the K–Ar dates, which are older than the eruption ages determined by the $^{40}Ar/^{39}Ar$ technique, may reflect the results related to alteration and inherited argon (Lo et al., 1994). $^{40}Ar/^{39}Ar$ dating in this study yielded the oldest eruption date at 17.1 ± 0.6 Ma (Table 3), which was considered to be the initial eruptive age. If this

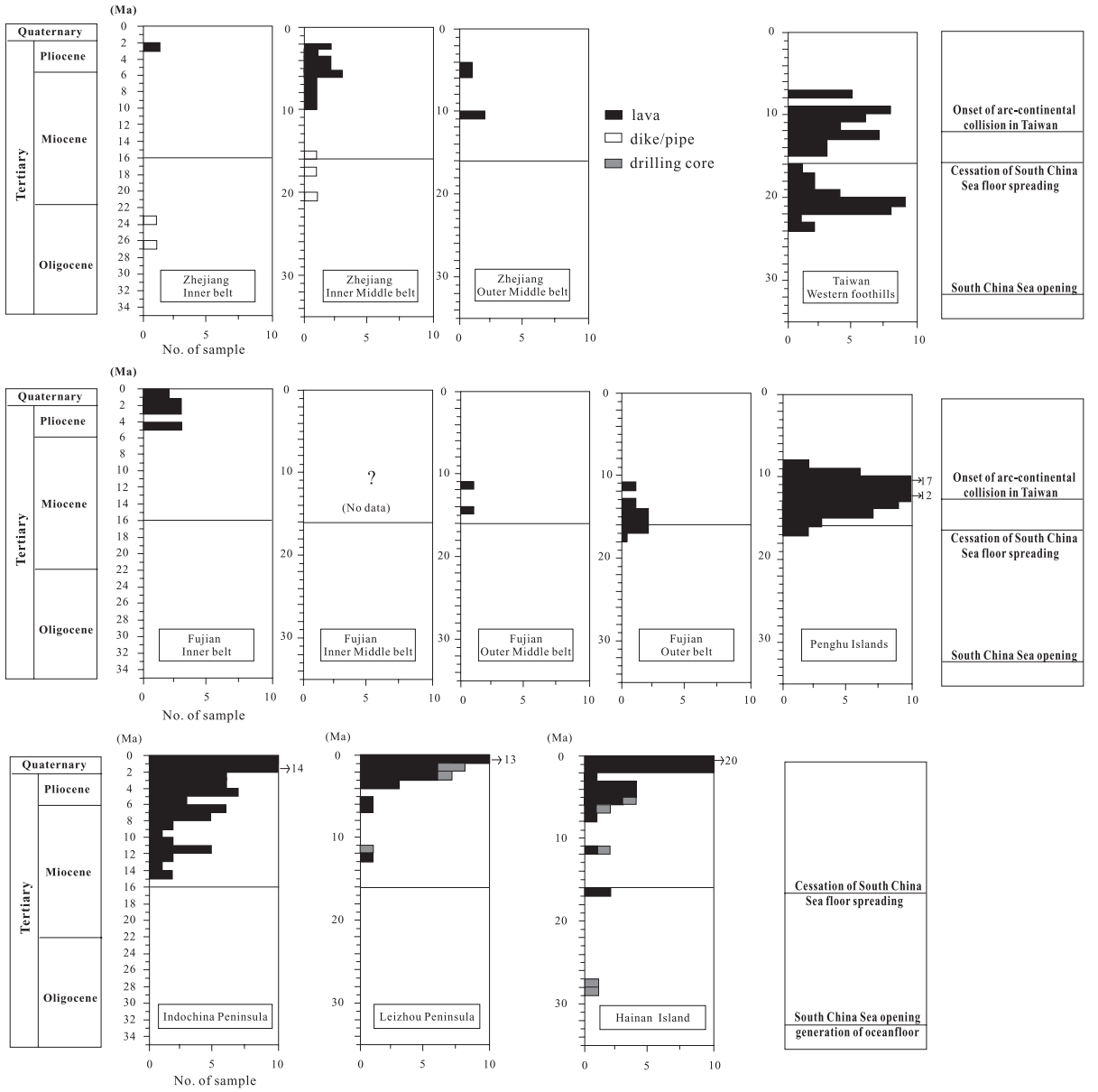

Fig. 13. Histogram showing ranges of radiometric ages for late Cenozoic basalts from four volcanic belts of Zhejiang–Fujian area, western foothills of Taiwan, Penghu Islands in the Taiwan Strait, Leizhou Peninsula, Hainan Island and Indochina Peninsula. Also shown are the major tectonic events in SE China. Age data of the basaltic rocks are compiled from the present study and the sources listed in Fig. 12 as well.

Ar–Ar age is accepted, it appears that the volcanic activity in the Zhejiang–Fujian area may start prior to 16 Ma.

Overall, volcanic activity began approximately 17 Ma ago at the eastern part of the Fujian province near the Longhai–Zhangpu region. Nine Ar–Ar ages (10.5–2.9 Ma) from the Outer Middle and Inner Middle belts of Zhejiang province are obtained in this study, which are roughly consistent with the previously reported K–Ar ages (10.4–4.8 Ma; Wang and Yang, 1987; Liu et al., 1992). These results support the observation that the volcanic rocks of these regions are younger than those of the Outer and Outer Middle belts of Fujian province (17.1–11.7 Ma). The volcanic activity of the Zhejiang province ceased about 2.5 Ma ago in the Zhuji area, while volcanism of Fujian Inner belt continued to be active until Quaternary (~ 0.72 Ma).

Generally speaking, the magmatism commenced and stopped, and eruption center migration in these regions may be influenced by the changing of tectonic setting. Intraplate melting could have resulted from rift-induced asthenospheric decompression during stress redistribution (Latin and White, 1990). Late Cenozoic intraplate basalts are widespread in the areas surrounding the South China Sea including Zhejiang–Fujian–Taiwan–eastern Guangdong, Leiqiong (including the Leizhou Peninsula and the northern of the Hainan Island), and Indochina Peninsula (Fig. 12). However, regional extensive intraplate magma occurred approximately following cessation of the South China Sea opening in these areas (Fig. 13). This implies that the eruption center of the basalts from the South China Sea mid-ocean ridge system might move northward (to Fujian Outer volcanic belt and Penghu Islands), northwestward (to the Leiqiong area) and westward (to south-central Vietnam) since the beginning of mid-Miocene (Fig. 12).

On the basis of the dating results and geographic distribution of the volcanic rocks, the inception and/or cessation of magmatic activity in the Zhejiang–Fujian region followed a rough time–space pattern, which appears to reflect progressive activation from Fujian Outer belt to western and northern-oriented rifts (Fig. 12). The western sector includes Minqing (14.1–11.9 Ma) and Mingxi (4.96–0.72 Ma), while the northern sector includes Shengxian–Xinchang (10.5–2.9 Ma) and Zhuji (2.5 Ma). Therefore, it is suggested that the cessation of magmatism and migration of eruption center in the Zhejiang–Fujian area may be related to the collision of Philippine Sea Plate with the Eurasian Plate during late Miocene to Quaternary.

About 12 Ma ago, the northern tip of the Luzon Arc might have begun overriding the Asian continental margin (Teng, 1992), and the present Taiwan area also began to experience compressional process. During Pliocene to Pleistocene, the collision event and the accompanying continental crust compression caused an active orogeny, which developed regional uplifting to form the mountain ranges in Taiwan. In late Cenozoic time, the regional extensional stress in the Taiwan area and its neighboring South China continental margin had been changed to compressive stress (Sun, 1985; Angelier et al., 1990). Therefore, although folding and thrusting diminished in intensity from east to west, and the orogenic records by arc–continental collision such as metamorphism and structural deformation were only restricted to the Taiwan area, whereas the intensified collision between the Luzon Island Arc and the continent of Asia during the ongoing convergence of the Eurasian and Philippine Sea plates might affect deep stress system of neighboring South China continental margin including Zhejiang–Fujian region. The youngest radiometric age of basaltic lava in each region might constrain the closure time of the magma-ascending related to compressive stress process. The igneous activity in the Fujian Outer belt ceased earlier than the Penghu Islands and western foothills of Taiwan which may be due to the fact that the coastal region of Fujian Province lies on the locus of upwelling, where the thickness of lithosphere (~ 80 km; Ma and Wu, 1987) is thinner than around the Penghu Islands (~ 100 km; Chung et al., 1994).

7. Conclusions

Late Cenozoic basaltic rocks in Zhejiang–Fujian area show wide variations in chemistry, ranging from tholeiitic to alkalic and strongly alkalic affinity. The chemical trends of major and trace elements in the basaltic rocks reveal that the fractional crystallization of clinopyroxene and olivine or plagioclase is the most important process during magma evolution. The chondrite-normalized REE abundances in the basaltic rocks have LREE-enriched patterns and the $(La/Yb)_N$ ratios

range from 4.9 to 42.9, which show strong resemblance to oceanic island basalts. In addition, the Sr–Nd–Pb isotopic component of basaltic rocks in Zhejiang–Fujian area showed an EM2 Dupal-type Pb signature. These geochemical features of the Zhejiang–Fujian basalts resemble those of other basaltic rocks occurred in SE China region. The chemical and isotopic data suggested that basaltic rocks were generated by mixing of different proportions of depleted asthenosphere (N-MORB) with enriched (EM2) mantle component.

Ar–Ar dating of 24 basaltic samples from the Zhejiang–Fujian area shows ages ranging from 0.9 to 26.4 Ma, providing good constraints on the timing of magmatic activity. These data, except some nephelinitic and basanitic pipes or dikes in the Inner belt of Zhejiang province, indicate that most basaltic magmatism occurred from 0.9 to 17.1 Ma in Zhejiang–Fujian area. According to the dating results, most late Cenozoic intraplate magmatism of SE China may be related to the northward migration of the South China Sea mid-ocean ridge system beneath SE China since the beginning of mid-Miocene, i.e., following cessation of the South China Sea opening. In Zhejiang–Fujian area, mid-Miocene volcanic activity is believed to start in the Outer belt, close to Longhai area in Fujian province. Owing to the collision of Philippine Sea Plate with the Eurasian Plate around Taiwan area in late Miocene (~ 12 Ma), the thermal centers gradually migrated westward and northward with time. The Zhuji (2.5 Ma) and Mingxi–Qingliu (0.7–5.0 Ma) volcanic eruptions are likely to be the latest.

Acknowledgements

We thank C. Hu for his assistance in the field. The Sr–Nd isotopic analysis was carried out by A.D. Smith and L.Y. Huang. The authors are most grateful for their kind assistance. Thanks are also due to P.L. Wang and L.H. Lin for their helpful assistance in the Ar–Ar dating and M. W. Hong for preparing the figures and typing the tables. We would like to thank Dr. Haibo Zou and an anonymous reviewer for their penetrating reviews that lead to significant improvement of the manuscript. This research was supported by the National Science Council, R.O.C., and the National Museum of Natural Science, Taichung, Taiwan. **[RR]**

References

Angelier, J., Bergerat, F., Chu, H.T., Juang, W.S., Lu, C.Y., 1990. Paleostress analysis as a key to margin extension: the Penghu Islands, South China Sea. Tectonophysics 183, 161–176.

Arvanne, S.E., Balogh, K., Nguyen, V.Q., Ravasz, C., Ravaszne-Baranyai, L., 1990. Magmatectonic relations and K/Ar dating of the basaltic rocks in the region of Bao Loc and Di Linh (South Vietnam). AMAll Foldt. Intez. Evi Jel. Az. I, 486–496 (Rez, Budapest, in Hungarian).

Barr, S.M., MacDonald, A.S., 1981. Geochemistry and geochronology of late Cenozoic basalts of Southeast Asia. Geol. Soc. Amer. Bull. (Part II) 92, 1069–1142.

Basu, A.R., Wang, J.W., Huang, W.K., Xie, G.H., Tatsumoto, M., 1991. Major element, REE and Pb, Nd and Sr isotopic geochemistry of Cenozoic volcanic rocks of eastern China: implication for their origin from sub-oceanic type mantle reservoirs. Earth Planet. Sci. Lett. 105, 149–169.

Briais, A., Patriat, P., Tapponnier, P., 1993. Updated interpretation of magnetic anomalies and seafloor spreading stages in the South China Sea: implications for the Tertiary tectonics of Southeast Asia. J. Geophys. Res. 98, 6299–6328.

Bureau of Geology and Mineral Resources of Fujian Province, 1985. Regional Geology of Fujian Province. Geological Publishing House, Beijing. 671 pp. In Chinese.

Bureau of Geology and Mineral Resources of Zhejiang Province, 1989. Regional Geology of Zhejiang Province. Geological Publishing House, Beijing. 688 pp. In Chinese.

Chen, C.H., 1990. Igneous Rocks in TaiwanThe Geology of Taiwan, vol. 1. Central Geol. Surv., MOEA, ROC. 137 pp. In Chinese.

Chih, C.S., 1988. The Study of Cenozoic Basalts and the Upper Mantle Beneath Eastern China (Attachment: Kimberlites). China Geosciences Univ. Press, Wuhan. 277 pp. In Chinese.

Chung, S.L., Sun, S.S., 1992. A new genetic model for the East Taiwan Ophiolite and its implications for Dupal domains in the northern hemisphere. Earth Planet. Sci. Lett. 109, 133–145.

Chung, S.L., Sun, S.S., Tu, K., Chen, C.H., Lee, C.Y., 1994. Late Cenozoic basaltic volcanism around the Taiwan Strait, SE China: product of lithosphere–asthenosphere interaction during continental extension. Chem. Geol. 112, 1–20.

Chung, S.L., Yang, T.F., Chen, S.J., Chen, C.H., Lee, T., Chen, C.H., 1995. Sr–Nd isotope compositions of high-pressure megacrysts and a lherzite inclusion in alkali basalts from western Taiwan. J. Geol. Soc. China 38 (1), 15–24.

Chung, S.L., Cheng, H., Jahn, B.M., O'Reilly, S.Y., Zhu, B., 1997. Major and trace element, and Sr–Nd isotope constraints on the origin of Paleogene volcanism in South China prior to the South China Sea opening. Lithos 40, 203–220.

Fan, Q.C., Hooper, P.R., 1989. The mineral chemistry of ultramafic xenoliths of eastern China: implications for upper mantle composition and the paleogeotherms. J. Petrol. 30, 1117–1158.

Fuhrmann, U., Lippolt, H.J., Hess, J.C., 1987. Examination of some proposed K–Ar standards: $^{40}Ar/^{39}Ar$ analyses and conventional K–Ar dating. Chem. Geol., Isot. Geosci. Sect. 66, 41–51.

Ge, T.M., Chen, W.J., Xu, X., Lee, D.M., Fan, L.M., Lee, Q., Wen, S.Y., Wang, X., 1989. The geomagnetic polarity time scale of

Quaternary for Leiqiong area—K–Ar dating and palaeomagnetic evidence from volcanic rocks. Acta Geophys. Sin. 32, 550–557 (in Chinese).

Govindaraju, K., 1994. 1994 compilation of working values and sample description for 383 geostandards. Geostand. Newsl. 18, 1–158.

Hart, S.R., Allegre, C.J., 1980. Trace element constraints on magma genesis. In: Hargraves, R.B. (Ed.), Physics of Magmatic Processes. Princeton Univ. Press, Princeton, NJ, pp. 121–139.

Hart, S.R., Gerlach, D.C., White, W.M., 1986. A possible new Sr–Nd–Pb mantle array and consequences for mantle mixing. Geochim. Cosmochim. Acta 50, 1551–1557.

Ho, K.S., 1998. Petrology and geochemistry of Cenozoic basalts from southern China. PhD thesis, Inst. Oceanog., National Taiwan Univ. 580 pp. (in Chinese with English abstract).

Ho, K.S., 1999. Sr–Nd isotope and geochemical evidence for the origin of clinopyroxene, amphibole and mica megacrysts in alkali basaltic rocks from southeastern China and Penghu Islands. Bull. Natl. Mus. Nat. Sci. 12, 1–31.

Ho, K.S., Chen, J.C., Juang, W.S., 2000a. Geochronology and geochemistry of late Cenozoic basalts from the Leiqiong area, Southern China. J. Asian Earth Sci. 18, 307–324.

Ho, K.S., Chen, J.C., Smith, A.D., Juang, W.S., 2000b. Petrogenesis of two groups of pyroxenite from Tungchihsu, Penghu Islands, Taiwan Strait: implications for mantle metasomatism beneath SE China. Chem. Geol. 167, 355–372.

Irving, A.J., 1984. Polybaric mixing and fractionation of alkalic magma: evidence from megacryst suites. EOS 65, 1153.

Jahn, B.M., 1986. Mid-ocean ridge or marginal basin origin of the East Taiwan Ophiolite: chemical and isotopic evidence. Contrib. Mineral. Petrol. 92, 194–206.

Juang, W.S., 1996. Geochronology and geochemistry of basalts in the Western Foothills, Taiwan. Bull. Natl. Mus. Nat. Sci. 7, 45–98.

Juang, W.S., Chen, J.C., 1992. Geochronology and geochemistry of Penghu basalts, Taiwan Strait and their tectonic significance. J. Southeast Asian Earth Sci. 7 (2/3), 185–193.

Lan, C.Y., Chung, S.L., Mertzman, S.A., Hsu, W.Y., 1994. Petrology, geochemistry and Nd–Sr isotope of late Miocene basalts in Liehyu and Chinmen, Fujian. J. Geol. Soc. China 37 (3), 309–334.

Lanphere, M.A., Dalrymple, G.B., 1978. The use of $^{40}Ar/^{39}Ar$ data in evaluation of disturbed K–Ar systems. Open-file Rep. (U. S. Geol. Surv.) 78-701, 241–243.

Latin, D., White, N., 1990. Generating melt during lithospheric extension: pure shear vs. simple shear. Geology 18, 327–331.

LaTourrette, T., Hervig, R.L., Holloway, J.R., 1995. Trace element partitioning between amphibole, phlogopite, and basanite melt. Earth Planet. Sci. Lett. 135, 13–30.

Le Bas, M.J., 1987. Nephelinites and carbonatites. In: Fitton, J.G., Upton, B.G.J. (Eds.), Alkaline Igneous Rocks. Blackwell, London, pp. 53–83.

Le Bas, M.J., 2000. IUGS reclassification of the high-Mg and picritic volcanic rocks. J. Petrol. 41, 1467–1470.

Lee, C.Y., 1994. Chronology and geochemistry of basaltic rocks from Penghu Islands and mafic dikes from east Fujian: implications for mantle evolution of SE China since late Mesozoic. PhD thesis, Inst. Geology, National Taiwan Univ. 233 pp. (in Chinese with English abstract).

Lee, T.Y., Lo, C.H., Chung, S.L., Chen, C.Y., Wang, P.L., Lin, W.P., Nguyen, H., Cung, T.C., Nguyen, T.Y., 1998. $^{40}Ar/^{39}Ar$ dating result of Neogene basalts in Vietnam and its tectonic implication. In: Flower, M.F.J., Chung, S.L., Lo, C.H., Lee, T.Y. (Eds.), Mantle Dynamics and Plate Interactions in East Asia. Geodynamics Series, vol. 27. American Geophysical Union Press, Washington, D.C., pp. 317–330.

Liu, R.X., Chen, W.J., Sun, J.Z., Li, D.M., 1992. The K–Ar age and tectonic environment of Cenozoic rock in China. In: Liu, R.X. (Ed.), The Age and Geochemistry of Cenozoic Volcanic Rock in China. Seismic Press, Beijing, pp. 1–43. In Chinese.

Liu, C.Q., Masuda, A., Xie, G.H., 1994. Major- and trace-element compositions of Cenozoic basalts in eastern China: petrogenesis and mantle source. Chem. Geol. 114, 19–42.

Lo, C.H., Lee, C.Y., 1994. $^{40}Ar/^{39}Ar$ method of K–Ar age determination of geological samples using Tsing-Hua Open Pool (THOR) Reactor. J. Geol. Soc. China 37 (1), 1–22.

Lo, C.H., Onstott, T.C., Chen, C.H., Lee, T., 1994. An assessment of $^{40}Ar/^{39}Ar$ dating for the whole-rock volcanic samples from the Luzon Arc near Taiwan. Chem. Geol. 114, 157–178.

Ma, X., Wu, D., 1987. Cenozoic extensional tectonics in China. Tectonophysics 133, 243–255.

Middlemost, E.A.K., 1989. Iron oxidation ratios, norms and the classification of volcanic rocks. Chem. Geol. 77, 19–26.

Odin, G.S., et al., 1982. Interlaboratory standards for dating potassium–argon age determinations. In: Odin, G.S. (Ed.), Numerical Dating in Stratigraphy. Wiley, Chichester, pp. 123–149.

Peng, Z.C., Zartman, R.E., Futa, K., Chen, D.G., 1986. Pb, Sr and Nd isotopic systematics and chemical characteristics of Cenozoic basalts, eastern China. Chem. Geol., Isot. Geosci. Sect. 59, 3–33.

Philpotts, J.A., Schnetzler, C.C., 1968. Europium anomalies and the genesis of basalts. Chem. Geol. 3, 5–13.

Qi, Q., Taylor, L.A., Zhou, X., 1995. Petrology and geochemistry of mantle peridotite xenoliths from SE China. J. Petrol. 36, 55–79.

Rangin, C., Huchon, P., Le Pichon, X., Bellon, H., Lepvrier, C., Roques, D., Hoe, N.D., Quynh, P.V., 1995. Cenozoic deformation of central and south Vietnam. Tectonophysics 251, 179–196.

Smith, A.D., 1998. The geodynamic significance of the DUPAL anomaly in Asia. In: Flower, M.F.J., Chung, S.L., Lo, C.H., Lee, T.Y. (Eds.), Mantle Dynamics and Plate Interactions in East Asia. Geodynamics Series, vol. 27. American Geophysical Union Press, Washington, D.C., pp. 89–105.

Smith, A.D., Huang, L.Y., 1997. The use of extraction chromatographic materials in procedures for the isotopic analysis of neodymium and strontium in rocks by thermal ionisation mass spectrometry. J. Natl. Cheng-Kung Univ. Sci. Eng. Med. Sect. 32, 1–10.

Staudigel, H., Zindler, A., Hart, S.R., Leslie, T., Chen, C.Y., Clague, D., 1984. The isotope systematic of a juvenile intraplate volcano: Pb, Nd and Sr isotope ratios of basalts from Loihi Seamount, Hawaii. Earth Planet. Sci. Lett. 69, 13–29.

Sun, S.C., 1985. The Cenozoic tectonic evolution of offshore Taiwan. Energy 10, 421–432.

Sun, J.S., 1991. Cenozoic volcanic activity in the northern South China Sea and Guangdong coastal area. Mar. Geol. Quat. Geol. 11, 45–67 (in Chinese).

Sun, S.S., Hanson, G.N., 1975. Origin of Ross Island basanitoids and limitations upon the heterogeneity of mantle source for alkali basalts and nephelinites. Contrib. Mineral. Petrol. 53, 77–106.

Sun, W., Lai, Z., 1980. Petrochemical characteristics of Cenozoic volcanic rocks in Fujian province and its relationship to tectonics. Geochimica 2, 134–147 (in Chinese).

Sun, S.S., McDonough, W.F., 1989. Chemical and isotopic systematics of oceanic basalts: implications for mantle composition and processes. J. Geol. Soc. Lond. Spec. Publ. 42, 313–345.

Taylor, B., Hayes, D.E., 1983. Origin and history of the South China Basin. In: Hayes, D.E. (Ed.), Tectonic and Geologic Evolution of Southeast Asian Seas and Islands, Part 2. AGU Geophys. Monogr. Ser., vol. 27, pp. 23–56.

Teng, L.S., 1992. Geotectonic evolution of Tertiary continental margin basins of Taiwan. Petrol. Geol. Taiwan 27, 1–19.

Tu, K., Flower, M.F.J., Carlson, R.W., Zhang, M., Xie, G., 1991. Sr, Nd and Pb isotopic compositions of Hainan Basalts (South China): implications for subcontinental lithosphere Dupal source. Geology 19, 567–569.

Tu, K., Flower, M.F.J., Carlson, R.W., Xie, G.H., Chen, C.Y., Zhang, M., 1992. Magmatism in the South China Basin: 1. Isotopic and trace element evidence for an endogenous Dupal mantle component. Chem. Geol. 97, 47–63.

Wang, R., Yang, S., 1987. Research on Cenozoic basalts and inclusions in Shengxian–Xinchang counties, Zhejiang province. Earth Sci. - J. Wuhan Coll. Geol. 12 (3), 241–248 (in Chinese).

Wilson, M., 1989. Igneous Petrogenesis. Harper Collins Academic, London. 466 pp.

Yoder, H.S., Tilley, C.E., 1962. Origin of basalt magmas: an experimental study of natural and synthetic rock system. J. Petrol. 3, 346–532.

York, D., 1969. Least-squares fitting of a straight line with correlated errors. Earth Planet. Sci. Lett. 5, 320–324.

Zhang, J.B., Chen, D.G., 1992. The geochemistry of basalts from Longhai and Mingxi areas in Fujian province. In: Liu, R.X. (Ed.), The Age and Geochemistry of Cenozoic Volcanic Rock in China. Seismic Press, Beijing, pp. 298–319. In Chinese.

Zhang, M., Tu, K., Xie, G.H., Flower, M.F.J., 1996. Subduction-modified subcontinental mantle in South China: trace element and isotope evidence in basalts from Hainan Island. Chin. J. Geochem. 15 (1), 1–19.

Zhao, H.L., 1990. Neogene–Quaternary Continental Rifting Volcanism and Deep Process in the Southeast Coast of China. China Geosciences Univ. Press, Wuhan. 163 pp. In Chinese.

Zhu, B.Q., Wang, H.F., 1989. Nd–Sr–Pb isotopic and chemical evidence for the volcanism with MORB-OIB source characteristics in the Leiqiong area, China. Geochimica 3, 193–201 (in Chinese).

Zindler, A., Hart, S.R., 1986. Chemical geodynamics. Annu. Rev. Earth Planet. Sci. Lett. 14, 493–571.

Zou, H., Zindler, A., Xu, X., Qi, Q., 2000. Major, trace element, and Nd, Sr and Pb isotope studies of Cenozoic basalts in SE China: mantle sources, regional variations, and tectonic significance. Chem. Geol. 171, 33–47.